

This is a repository copy of *The atmospheric impacts of monoterpene ozonolysis on global stabilised Criegee intermediate budgets and SO<sub>2</sub> oxidation: experiment, theory and modelling*.

White Rose Research Online URL for this paper:

<https://eprints.whiterose.ac.uk/125067/>

Version: Published Version

---

**Article:**

Newland, M. J., Rickard, A. R. [orcid.org/0000-0003-2203-3471](https://orcid.org/0000-0003-2203-3471), Sherwen, T. [orcid.org/0000-0002-3006-3876](https://orcid.org/0000-0002-3006-3876) et al. (5 more authors) (2018) The atmospheric impacts of monoterpene ozonolysis on global stabilised Criegee intermediate budgets and SO<sub>2</sub> oxidation: experiment, theory and modelling. *Atmospheric Chemistry and Physics*. pp. 6095-6120. ISSN 1680-7324

<https://doi.org/10.5194/acp-18-6095-2018>

---

**Reuse**

This article is distributed under the terms of the Creative Commons Attribution (CC BY) licence. This licence allows you to distribute, remix, tweak, and build upon the work, even commercially, as long as you credit the authors for the original work. More information and the full terms of the licence here:

<https://creativecommons.org/licenses/>

**Takedown**

If you consider content in White Rose Research Online to be in breach of UK law, please notify us by emailing [eprints@whiterose.ac.uk](mailto:eprints@whiterose.ac.uk) including the URL of the record and the reason for the withdrawal request.



# The atmospheric impacts of monoterpene ozonolysis on global stabilised Criegee intermediate budgets and SO<sub>2</sub> oxidation: experiment, theory and modelling

Mike J. Newland<sup>1,3</sup>, Andrew R. Rickard<sup>2,3</sup>, Tomás Sherwen<sup>3</sup>, Mathew J. Evans<sup>2,3</sup>, Luc Vereecken<sup>4,5</sup>, Amalia Muñoz<sup>6</sup>, Milagros Ródenas<sup>6</sup>, and William J. Bloss<sup>1</sup>

<sup>1</sup>University of Birmingham, School of Geography, Earth and Environmental Sciences, Birmingham, UK

<sup>2</sup>National Centre for Atmospheric Science (NCAS), University of York, York, UK

<sup>3</sup>Wolfson Atmospheric Chemistry Laboratories, Department of Chemistry, University of York, York, UK

<sup>4</sup>Max Planck Institute for Chemistry, Atmospheric Sciences, Hahn-Meitner-Weg 1, Mainz, Germany

<sup>5</sup>Institute for Energy and Climate Research, Forschungszentrum Jülich GmbH, Jülich, Germany

<sup>6</sup>Fundación CEAM, EUPHORE Laboratories, Avda/Charles R. Darwin 14. Parque Tecnológico, Valencia, Spain

**Correspondence:** Mike J. Newland (mike.newland@york.ac.uk) and Andrew R. Rickard (andrew.rickard@york.ac.uk)

Received: 24 November 2017 – Discussion started: 5 December 2017

Revised: 7 March 2018 – Accepted: 13 April 2018 – Published: 2 May 2018

**Abstract.** The gas-phase reaction of alkenes with ozone is known to produce stabilised Criegee intermediates (SCIs). These biradical/zwitterionic species have the potential to act as atmospheric oxidants for trace pollutants such as SO<sub>2</sub>, enhancing the formation of sulfate aerosol with impacts on air quality and health, radiative transfer and climate. However, the importance of this chemistry is uncertain as a consequence of limited understanding of the abundance and atmospheric fate of SCIs. In this work we apply experimental, theoretical and numerical modelling methods to quantify the atmospheric impacts, abundance and fate of the structurally diverse SCIs derived from the ozonolysis of monoterpenes, the second most abundant group of unsaturated hydrocarbons in the atmosphere. We have investigated the removal of SO<sub>2</sub> by SCIs formed from the ozonolysis of three atmospherically important monoterpenes ( $\alpha$ -pinene,  $\beta$ -pinene and limonene) in the presence of varying amounts of water vapour in large-scale simulation chamber experiments that are representative of boundary layer conditions. The SO<sub>2</sub> removal displays a clear dependence on water vapour concentration, but this dependence is not linear across the range of [H<sub>2</sub>O] explored. At low [H<sub>2</sub>O] a strong dependence of SO<sub>2</sub> removal on [H<sub>2</sub>O] is observed, while at higher [H<sub>2</sub>O] this dependence becomes much weaker. This is interpreted as being caused by the production of a variety of structurally (and hence chemically) different SCIs in each of the systems studied, which dis-

played different rates of reaction with water and of unimolecular rearrangement or decomposition. The determined rate constants,  $k(\text{SCI}+\text{H}_2\text{O})$ , for those SCIs that react primarily with H<sub>2</sub>O range from 4 to  $310 \times 10^{-15} \text{ cm}^3 \text{ s}^{-1}$ . For those SCIs that predominantly react unimolecularly, determined rates range from 130 to  $240 \text{ s}^{-1}$ . These values are in line with previous results for the (analogous) stereo-specific SCI system of *syn-anti*-CH<sub>3</sub>CHOO. The experimental results are interpreted through theoretical studies of the SCI unimolecular reactions and bimolecular reactions with H<sub>2</sub>O, characterised for  $\alpha$ -pinene and  $\beta$ -pinene at the M06-2X/aug-cc-pVTZ level of theory. The theoretically derived rates agree with the experimental results within the uncertainties. A global modelling study, applying the experimental results within the GEOS-Chem chemical transport model, suggests that > 97 % of the total monoterpene-derived global SCI burden is comprised of SCIs with a structure that determines that they react slowly with water and that their atmospheric fate is dominated by unimolecular reactions. Seasonally averaged boundary layer concentrations of monoterpene-derived SCIs reach up to  $1.4 \times 10^4 \text{ cm}^{-3}$  in regions of elevated monoterpene emissions in the tropics. Reactions of monoterpene-derived SCIs with SO<sub>2</sub> account for < 1 % globally but may account for up to 60 % of the gas-phase SO<sub>2</sub> removal over areas of tropical forests, with significant localised impacts on

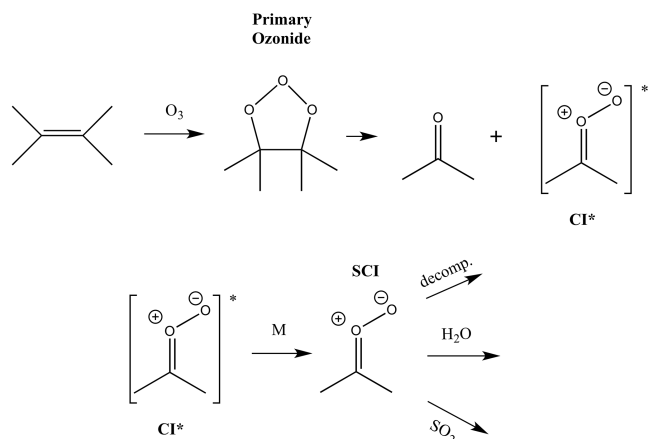
the formation of sulfate aerosol and hence the lifetime and distribution of  $\text{SO}_2$ .

## 1 Introduction

Chemical oxidation processes in the atmosphere exert a major influence on atmospheric composition, leading to the removal of primary emitted species and the formation of secondary products. In many cases either the emitted species or their oxidation products negatively impact air quality and climate (e.g. ozone, which is also a potent greenhouse gas). These reactions can also transform gas-phase species to the condensed phase, forming secondary aerosol that again can be harmful to health and can both directly and indirectly influence radiative transfer and hence climate (e.g.  $\text{SO}_2$  oxidation leading to the formation of sulfate aerosol).

Tropospheric gas-phase oxidants include the OH radical, ozone, the  $\text{NO}_3$  radical and halogen atoms. Stabilised Criegee intermediates (SCIs), or carbonyl oxides, have been identified as another potentially important oxidant in the troposphere (e.g. Cox and Penkett, 1971; Mauldin III et al., 2012). SCIs are thought to be formed in the atmosphere predominantly from the reaction of ozone with unsaturated hydrocarbons, though other processes may be important under certain conditions, e.g. alkyl iodide photolysis (Gravestock et al., 2010), dissociation of the DMSO peroxy radical (Asatryan and Bozzelli, 2008). Laboratory experiments and theoretical calculations have shown SCIs to oxidise  $\text{SO}_2$  (e.g. Cox and Penkett, 1971; Welz et al., 2012; Taatjes et al., 2013), organic (Welz et al., 2014) and inorganic (Foreman et al., 2016) acids (Vereecken, 2017) and a number of other important trace gases found in the atmosphere, as well as forming adducts with  $\text{NO}_2$  (Taatjes et al., 2014; Vereecken and Nguyen, 2017; Caravan et al., 2017). Measurements in a boreal forest (Mauldin III et al., 2012) and at a coastal site (Berresheim et al., 2014) have both identified a missing process (in addition to a reaction with OH) that oxidises  $\text{SO}_2$  to  $\text{H}_2\text{SO}_4$ , potentially arising from SCI reactions.

Here, we present results from a series of experimental studies into SCI formation and reactions, carried out under atmospheric boundary layer conditions in the European Photochemical Reactor facility (EUPHORE), Valencia, Spain. We examine the ozonolysis of three monoterpenes with very different structures (and hence reactivities with OH and ozone):  $\alpha$ -pinene (with an endocyclic double bond),  $\beta$ -pinene (with an exocyclic double bond) and limonene (with both an endo- and exocyclic double bond). We observe the removal of  $\text{SO}_2$  in the presence of each alkene–ozone system as a function of water vapour concentration. This allows us to derive relative SCI kinetics for reaction with  $\text{H}_2\text{O}$ ,  $\text{SO}_2$  and unimolecular decomposition. Further, we calculate absolute unimolecular rates and bimolecular reaction rates with  $\text{H}_2\text{O}$  for all  $\alpha$ -pinene- and  $\beta$ -pinene-derived SCIs at the M06-



**Scheme 1.** Simplified generic mechanism for the reaction of Criegee intermediates (CIs) formed from alkene ozonolysis.

2X/aug-cc-pVTZ level of theory. A global modelling study, using the GEOS-Chem global chemical transport model, is performed to assess global and regional impacts of the chemical kinetics of monoterpene SCIs determined in this study.

### 1.1 Stabilised Criegee intermediate kinetics

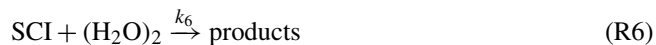
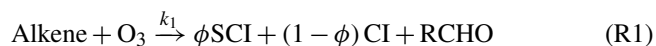
Ozonolysis of an unsaturated hydrocarbon produces a primary ozonide that rapidly decomposes to yield pairs of Criegee intermediates (CIs) and carbonyls (Johnson and Marston, 2008). The population of CIs are formed with a broad internal energy distribution, giving both chemically activated and stabilised forms. Chemically activated CIs may undergo collisional stabilisation to an SCI, unimolecular decomposition or isomerisation. SCIs can have sufficiently long lifetimes in which to undergo bimolecular reactions (Scheme 1).

The predominant atmospheric fate for the simplest SCI,  $\text{CH}_2\text{OO}$ , is reaction with water vapour, which likely occurs with the dimer ( $(\text{H}_2\text{O})_2$ ) (e.g. Berndt et al., 2014; Newland et al., 2015a; Chao et al., 2015; Lewis et al., 2015; Lin et al., 2016a). For larger SCI, both experimental (Taatjes et al., 2013; Sheps et al., 2014; Newland et al., 2015a; Huang et al., 2015) and theoretical (Kuwata et al., 2010; Anglada et al., 2011; Anglada and Sole, 2016; Vereecken et al., 2017) studies have shown that their kinetics, in particular reaction with water, are highly structure dependent. The significant double-bond character exhibited in the zwitterionic configurations of mono-substituted SCIs leads to two distinct chemical forms: *syn*-SCIs (i.e. those where an alkyl substituent group is on the same side as the terminal oxygen of the carbonyl oxide moiety) and *anti*-SCIs (i.e. with the terminal oxygen of the carbonyl oxide moiety on the same side as a hydrogen group). The two conformers of  $\text{CH}_3\text{CHOO}$ , which are both mono-substituted, display these properties. This difference in conformer reactivities has been predicted

theoretically (Ryzhkov and Ariya, 2004; Kuwata et al., 2010; Anglada et al., 2011; Lin et al., 2016a) and was subsequently confirmed experimentally (Taatzjes et al., 2013; Sheps et al., 2014) for the two CH<sub>3</sub>CHO conformers. The significantly faster reaction of *anti*-CH<sub>3</sub>CHO with water is driven by the higher potential energy of this isomer, while more stable SCI, with a methyl group in *syn*-position, such as *syn*-CH<sub>3</sub>CHO or (CH<sub>3</sub>)<sub>2</sub>COO, react orders of magnitude more slowly with water.

To date, the effects of the water dimer, (H<sub>2</sub>O)<sub>2</sub> on SCI removal have only been determined experimentally for CH<sub>2</sub>OO (Berndt et al., 2014; Chao et al., 2015; Lewis et al., 2015; Newland et al., 2015a; Sheps et al., 2017; Liu et al., 2017) and *anti*-CH<sub>3</sub>CHO (Lin et al., 2016b). Theoretical calculations (Vereecken et al., 2017) have predicted the ratio of the SCI + (H<sub>2</sub>O)<sub>2</sub> : SCI + H<sub>2</sub>O rate constants,  $k_5/k_3$ , of larger and more substituted SCI to be of a similar order of magnitude as for CH<sub>2</sub>OO (i.e. 1.5–2.5 × 10<sup>3</sup>).

SCIs can also undergo unimolecular isomerisation or decomposition in competition with bimolecular reactions. This is likely to be a significant atmospheric sink for *syn*-SCIs because of their slow reaction with water vapour (e.g. Huang et al., 2015). Unimolecular reactions of *syn*-CI/SCIs are dominated by a 1,4-H shift, forming a vinyl hydroperoxide (VHP) intermediate (Niki et al., 1987; Rickard et al., 1999; Martinez and Herron, 1987; Johnson and Marston, 2008; Kidwell et al., 2016). Decomposition of the VHP formed in this process is an important non-photolytic source of OH, HO<sub>2</sub> and RO<sub>2</sub> in the atmosphere (Niki et al., 1987; Alam et al., 2013; Kidwell et al., 2016), which can also lead to secondary organic aerosol formation (Ehn et al., 2014). Unimolecular reactions of the *anti*-CI/SCIs are thought to be dominated by a 1,3-ring closure, the acid ester channel, in which the CI/SCI decomposes, through rearrangement to a dioxirane intermediate, producing a range of daughter products and contributing to the observed overall HO<sub>x</sub> radical yield (Kroll et al., 2002; Johnson and Marston, 2008; Alam et al., 2013).



Decomposition of the simplest SCI, CH<sub>2</sub>OO, is slow (< 10 s<sup>-1</sup>) and is not likely to be an important sink in the troposphere (e.g. Newland et al., 2015a; Chhantyal-Pun et al., 2015). This decomposition occurs primarily via rearrangement through a “hot” acid species, which represents the lowest accessible decomposition channel (Gutbrod et al., 1996; Alam et al., 2011; Chen et al.,

2016). However, recently determined unimolecular reaction rates of larger *syn*-SCIs are considerably faster. Newland et al. (2015a) reported unimolecular reaction rate constants for *syn*-CH<sub>3</sub>CHO of 348 (±332) s<sup>-1</sup> and for (CH<sub>3</sub>)<sub>2</sub>COO of 819 (±190) s<sup>-1</sup> (assuming  $k(\text{syn-CH}_3\text{CHO} + \text{SO}_2) = 2.9 \times 10^{-11} \text{ cm}^3 \text{ s}^{-1}$  (Sheps et al., 2014) and  $k((\text{CH}_3)_2\text{COO} + \text{SO}_2) = 1.3 \times 10^{-10} \text{ cm}^3 \text{ s}^{-1}$  (Huang et al., 2015), respectively). Smith et al. (2016) measured the unimolecular decomposition rate of (CH<sub>3</sub>)<sub>2</sub>COO to be 269 (±82) s<sup>-1</sup> at 283 K, increasing to 916 (±56) s<sup>-1</sup> at 323 K and suggesting the rate to be fast and highly temperature dependent. Novelli et al. (2014) estimated a significantly slower decomposition rate for *syn*-CH<sub>3</sub>CHO of 20 (3–30) s<sup>-1</sup> from direct observations of OH formation, while Fenske et al. (2000) estimated the decomposition rate of CH<sub>3</sub>CHO (i.e. a mix of *syn*- and *anti*-conformers) produced from ozonolysis of *trans*-but-2-ene to be 76 s<sup>-1</sup> (accurate to within a factor of 3).

## 1.2 Monoterpene ozonolysis

Monoterpenes are volatile organic compounds (VOCs) with the general formula C<sub>10</sub>H<sub>16</sub> and are emitted by a wide range of vegetation, but particularly from boreal forests. Total global monoterpene emissions are estimated to be 95 (±3) Tg yr<sup>-1</sup> (Sindelarova et al., 2014) – roughly 13 % of total non-methane biogenic VOC emissions. Monoterpene emissions are dominated by α-pinene, which accounts for roughly 34 % of the total global emissions, while β-pinene and limonene account for 17 and 9 % respectively (Sindelarova et al., 2014). Monoterpenes (mainly α-pinene and limonene) are also present in indoor environments, in significant amounts where cleaning products and air fresheners are in routine use (of the order of 100 s of ppbv) (e.g. Singer et al., 2006a, b; Sarwar and Corsi, 2007), and where their ozonolysis products can affect indoor chemistry and health (e.g. Rossignol et al., 2013; Shallcross et al., 2014).

Monoterpenes are highly reactive due to the presence of (often multiple) double bonds. The oxidation of monoterpenes yields a wide range of multi-functional gas-phase and aerosol products. This process can be initiated by OH and NO<sub>3</sub> radicals or by O<sub>3</sub>, with ozonolysis having been shown to be particularly efficient at generating low-volatility products that can form SOA, even in the absence of sulfuric acid (e.g. Ehn et al., 2014; Kirkby et al., 2016). These highly oxygenated secondary products have received considerable attention in recent years because of their role in affecting the climate through absorption and scattering of solar radiation (the direct aerosol effect). They can also increase cloud condensation nuclei concentrations, which can change cloud properties and lifetimes (the indirect aerosol effect). They have also been shown to have a wide range of deleterious effects on human health (e.g. Pöschl and Shiraiwa, 2015).

The ozonolysis reaction for monoterpenes is expected to follow a similar initial process to that of smaller alkenes,

with cyclo-addition at a double bond giving a primary ozonide (POZ), followed by rapid decomposition of the POZ to yield a CI and a carbonyl (Scheme 1). Stabilisation of the large POZs formed in monoterpene ozonolysis is expected to be negligible (Nguyen et al., 2009a). However, a major difference in ozonolysis at endocyclic bonds is that, on decomposition of the POZ, the carbonyl oxide and carbonyl moieties are tethered as part of the same molecule, providing the potential for further interaction of the two. These can react together to form secondary ozonides (SOZ), which may be stable for several hours (Beck et al., 2011). However, while this has been shown to be potentially the major fate in the atmosphere for SCIs derived from sesquiterpenes ( $C_{15}H_{24}$ ) (e.g. Nguyen et al., 2009b; Beck et al., 2011; Yao et al., 2014), formation of SOZ is predicted to be small for monoterpene-derived SCIs because of the high ring strain caused by the tight cyclisation (e.g. Nguyen et al., 2009b). Chuong et al. (2004) predicted formation of a SOZ to become the dominant atmospheric fate for SCIs formed in the ozonolysis of endocyclic alkenes with a carbon number between 8 and 15, while Vereecken and Francisco (2012) suggested that internal SOZ formation is likely to be limited to product rings containing six or more carbons due to ring strain.

No studies have yet directly determined the reaction rates of the large SCIs produced from monoterpene ozonolysis with  $SO_2$  (or any other trace gases). This is owing to the complexities of synthesising and measuring large SCI. However, Ahrens et al. (2014) concluded that the reaction of the C9-SCI formed in  $\beta$ -pinene ozonolysis with  $SO_2$  is as fast as that determined by Welz et al. (2012) and Taatjes et al. (2013) for  $CH_2OO$  and  $CH_3CHOO$  respectively (ca.  $4 \times 10^{-11} \text{ cm}^3 \text{ s}^{-1}$ ) by fitting to the decay of  $SO_2$  in the presence of the ozonolysis reaction. Mauldin III et al. (2012) calculated significantly slower reaction rates for an additional oxidant (assumed to be SCI) derived from  $\alpha$ -pinene and limonene ozonolysis, with  $k(\text{SCI} + SO_2)$  determined to be  $6 \times 10^{-13}$  and  $8 \times 10^{-13} \text{ cm}^3 \text{ s}^{-1}$  for  $\alpha$ -pinene and limonene-derived SCIs respectively. However, it seems likely that the rates calculated by Mauldin III et al. (2012) may be substantially underestimated due to the assumption of a very long SCI lifetime (0.2 s) in experiments that were performed at 50 % RH. The calculated rates scale linearly with SCI lifetime, and based on reaction rates of smaller SCIs with  $H_2O$  (reported since the Mauldin III et al. work, e.g. Taatjes et al., 2013), it seems likely that the lifetime of the SCI in their experiments would have been more like  $0.1\text{--}2 \times 10^{-2} \text{ s}$ , increasing the calculated rate constants by more than an order of magnitude and bringing them into much closer agreement with the rates reported by Ahrens et al. (2014).

Unimolecular reactions of the monoterpene SCIs are expected to proceed rapidly through the VHP route if hydrogen is available for a 1,4-H shift. Those SCIs that cannot undergo this rearrangement may undergo unimolecular reactions via the formation of the dioxirane intermediate, but this is expected to be a much slower process (Nguyen et al., 2009a). In

contrast to smaller SCI, it has been observed experimentally and predicted theoretically that the VHP route will mainly lead to rearrangement into an acid (also yielding an OH radical) rather than decomposition of the molecule (e.g. Ma et al., 2008; Ma and Marston, 2008). As for the smaller alkenes, monoterpene ozonolysis has been shown to be a source of  $HO_x$  (e.g. Paulson et al., 1997; Alam et al., 2013), predominantly via the VHP rearrangement. The MCMv3.3.1 (Jenkin et al., 2015) applies OH yields of 0.80, 0.35 and 0.87 for  $\alpha$ -pinene,  $\beta$ -pinene and limonene respectively.

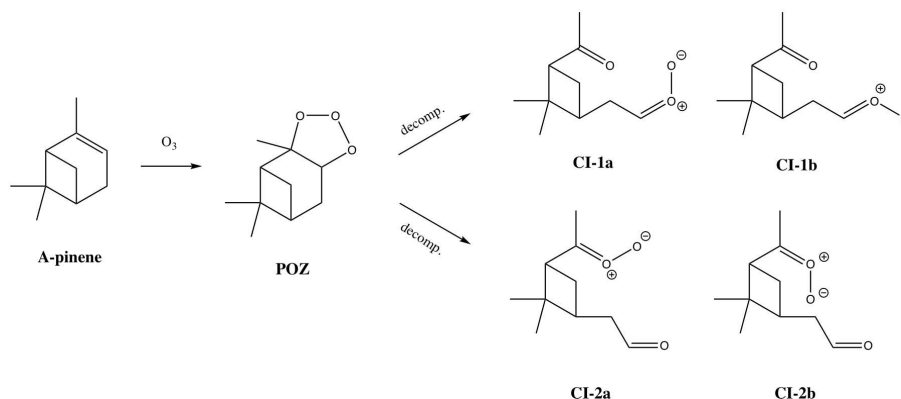
### 1.2.1 $\alpha$ -pinene-derived SCI

Decomposition of the  $\alpha$ -pinene POZ yields four different  $C_{10}$  Criegee intermediates (Scheme 2: CI-1a, 1b, 2a, 2b), with the carbonyl oxide moiety at one end and a carbonyl group at the other. Here, CI-1 is a mono-substituted CI for which both *syn*- (1a) and *anti*-conformers (1b) exist while the other, CI-2, is disubstituted and two *syn*-conformers (2a and 2b) exist for it. Ma et al. (2008) infer a relative yield of 50 % for the two basic CIs formed, based on the observation that nopinonic acid yields from the ozonolysis of  $\alpha$ -pinene and an enone, which upon ozonolysis yields CI-1, are almost indistinguishable.

The total SCI yield from  $\alpha$ -pinene was determined to be  $0.15 (\pm 0.07)$  by Sipilä et al. (2014) in indirect experiments measuring the production of  $H_2SO_4$  from  $SO_2$  oxidation in the  $\alpha$ -pinene ozonolysis system. Drozd and Donahue (2011) also determined a total SCI yield of about 0.15 at 740 Torr from measuring the loss of hydrofluoroacetone in ozonolysis experiments in a high-pressure flow system. The MCMv3.3.1 (Jenkin et al., 1997, 2015; Saunders et al., 2003) applies a value of 0.20 based on stabilisation of only the mono-substituted CI-1.

### 1.2.2 $\beta$ -pinene-derived SCI

$\beta$ -pinene ozonolysis yields two distinct conformers of the nopinone C9-CI (Scheme 3: CI-3 and CI-4), which differ in orientation of the carbonyl oxide group, and  $CH_2OO$ . CI-3 and CI-4 are formed in roughly equal proportions with very little interconversion between the two (Nguyen et al., 2009a). The difference in the chemical behaviour of CI-3 and CI-4, which were often not distinguished in earlier studies, arises from the inability of the carbon attached to the 4-membered ring to undergo the 1,4-H shift that allows unimolecular decomposition via the VHP channel. This was noted in Rickard et al. (1999) as being a reason for the considerably lower OH yield (obtained via the VHP route) from  $\beta$ -pinene ozonolysis compared to that of  $\alpha$ -pinene. This difference leads to contrasting unimolecular decomposition rates for the two CIs, with Nguyen et al. (2009a) predicting a loss rate of ca.  $50 \text{ s}^{-1}$  for CI-3 (via a VHP) and ca.  $1 \text{ s}^{-1}$  for CI-4 (via ring closure to a dioxirane). This result is qualitatively consistent with the experimental work of Ahrens et al. (2014), who deter-



**Scheme 2.** Mechanism of formation of the two Criegee intermediates (CIs) from  $\alpha$ -pinene ozonolysis.

mine a ratio of 85 : 15 for the abundance of SCI-4 : SCI-3 about 10 s after the initiation of the ozonolysis reaction, as a consequence of the much faster decomposition rate of SCI-3. The potential for bimolecular reactions to compete with decomposition of SCI-3 is very different from the potential for bimolecular reactions to compete with decomposition of SCI-4.

Nguyen et al. (2009a) theoretically calculate a total SCI yield from  $\beta$ -pinene ozonolysis of 42 %, consisting of 16.2 % SCI-3, 20.6 % SCI-4 and 5.1 %  $CH_2OO$ . Ahrens et al. (2014) assume an equal yield of CI-3 and CI-4 (45 %) with a 10 % yield of  $CH_2OO$ ; 40 % of the total C9-CI are calculated to be stabilised at 1 atm. If all of the  $CH_2OO$  is assumed to be stabilised when it is formed (e.g. Nguyen et al., 2009a), this gives a total SCI yield of 46 %. Earlier experimental studies have tended to determine lower total SCI yields, with Hasson et al. (2001) reporting a total SCI yield of 0.27 from measured product yields (almost entirely nopinone) and Hatakeyama et al. (1984) reporting a total SCI yield of 0.25. Winterhalter et al. (2000) determined a yield of 0.16 ( $\pm 0.04$ ) for excited  $CH_2OO$  from  $\beta$ -pinene ozonolysis, obtained via the nopinone yield and 0.35 for the stabilised C9-CI, giving a total SCI yield of 0.51 if all the  $CH_2OO$  is assumed to be stabilised. Also, experimental studies have tended to report higher  $CH_2OO$  yields (determined from measured nopinone yields) than theoretical studies. Nguyen et al. (2009a) note that this could be because nopinone can also be formed in bimolecular reactions of SCI-4, hence experimental studies may overestimate  $CH_2OO$  production. The MCMv3.3.1 incorporates a total SCI yield of 0.25 from  $\beta$ -pinene ozonolysis, with a yield of stabilised C9-CI of 0.102 and a  $CH_2OO$  yield of 0.148.

### 1.2.3 Limonene-derived SCI

Limonene has two double bonds with which ozone can react. Theory suggests that reaction at the endocyclic bond is more likely: Baptista et al. (2011) calculate the reaction at the endocyclic bond to be 84–94 % (dependent on the level

of theory applied). Zhang et al. (2006) suggest the reaction at the endocyclic double bond to be roughly 25 times faster than at the exocyclic bond, i.e. leading to a branching ratio of ca. 96 % reaction at the endobond and the current IUPAC recommendation (IUPAC, 2013) suggests about 95 % of the primary ozone reaction to be at the endobond. Leungsakul et al. (2005) reported a best fit to measurements from chamber experiments by assuming an 85 % reaction at the endocyclic bond and 15 % at the exocyclic bond.

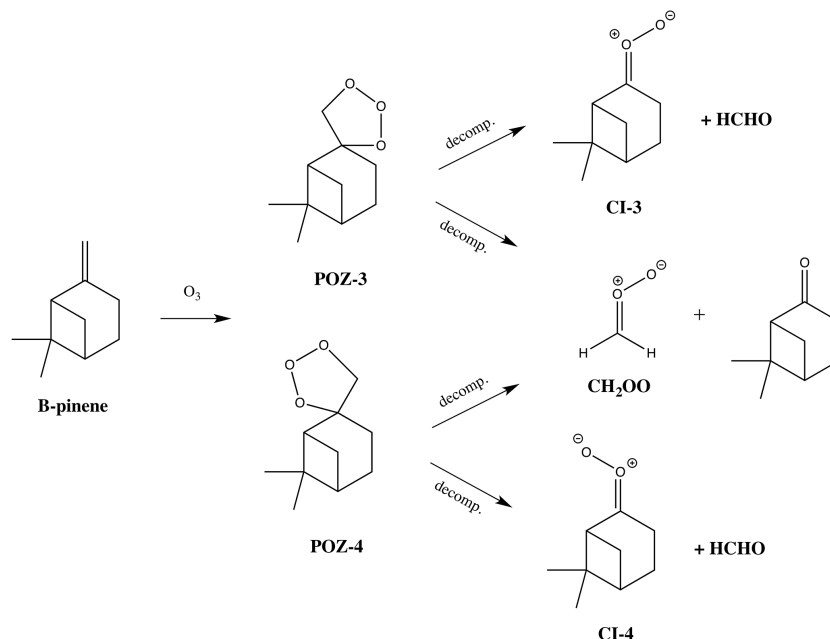
Ozone reaction at the endocyclic bond of limonene produces four different C<sub>10</sub> CIs (Scheme 4: CI-5a, 5b, 6a, 6b). Similarly to CI-1 and CI-2 from  $\alpha$ -pinene, CI-5 is a mono-substituted CI for which both *syn*- (5a) and *anti*- conformers (5b) exist, while the other, CI-6, is disubstituted, for which two *syn*-conformers (6a and 6b) exist. Leungsakul et al. (2005) determined a total SCI yield from limonene ozonolysis of 0.34, consisting of  $CH_2OO$  (0.05), CI-7 (0.04), CI-5 (0.15) and CI-6 (0.11). Sipilä et al. (2014) determined a total SCI yield of 0.27 ( $\pm 0.12$ ) from indirect experiments measuring the production of  $H_2SO_4$  from  $SO_2$  oxidation in the presence of the limonene–ozone system. The MCMv3.3.1 only describes reaction with ozone at the endocyclic double bond and recommends a total SCI yield of 0.135 with stabilisation of only the mono-substituted CI-5.

## 2 Experimental study

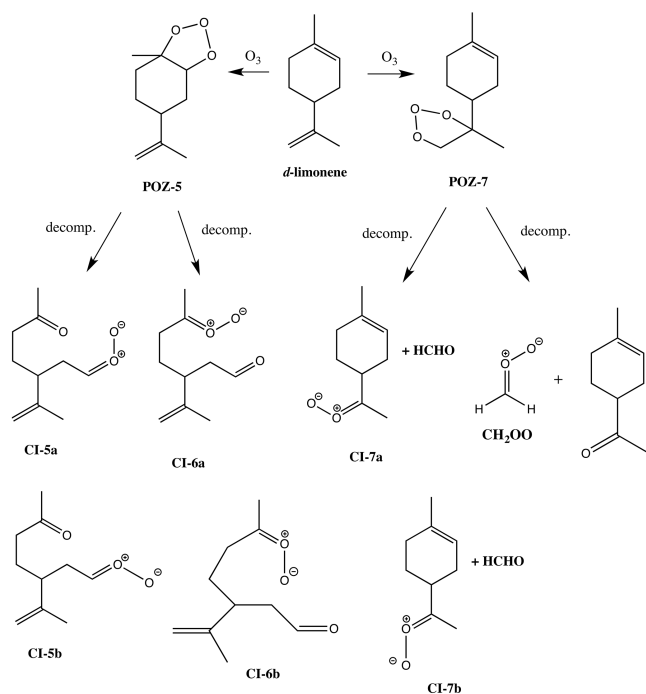
### 2.1 Experimental approach

The EUPHORE facility is a 200 m<sup>3</sup> simulation chamber used primarily for studying reaction mechanisms under atmospheric boundary layer conditions. Further details of the chamber set-up and instrumentation are available elsewhere (Becker, 1996; Alam et al., 2011), and a detailed account of the experimental procedure, summarised below, is given in Newland et al. (2015a).

Experiments comprised time-resolved measurements of the removal of  $SO_2$  in the presence of the monoterpene–



**Scheme 3.** Mechanism of formation of the three Criegee intermediates (CIs) from  $\beta$ -pinene ozonolysis.



**Scheme 4.** Mechanism of formation of the four Criegee intermediates (CIs) from limonene ozonolysis.

ozone system as a function of humidity.  $\text{SO}_2$  and  $\text{O}_3$  abundance were measured using conventional fluorescence (reported precision  $\pm 1.0$  ppbv) and UV absorption monitors (reported precision  $\pm 4.5$  ppbv), respectively; alkene abun-

dance was determined via FTIR spectroscopy. Experiments were performed in the dark (i.e. with the chamber housing closed;  $j(\text{NO}_2) \leq 10^{-6} \text{ s}^{-1}$ ), at atmospheric pressure (ca. 1000 mbar) and temperatures between 287 and 302 K. The chamber is fitted with large horizontal and vertical fans to ensure rapid mixing (ca. 2 min). Chamber dilution was monitored via the first-order decay of an aliquot of  $\text{SF}_6$ , added prior to each experiment. Cyclohexane (ca. 75 ppmv) was added at the beginning of each experiment to act as an OH scavenger, such that  $\text{SO}_2$  reaction with OH was calculated to be  $\leq 1\%$  of the total chemical  $\text{SO}_2$  removal in all experiments.

The experimental procedure, starting with the chamber filled with clean scrubbed air, comprised addition of  $\text{SF}_6$  and cyclohexane, followed by water vapour,  $\text{O}_3$  (ca. 500 ppbv) and  $\text{SO}_2$  (ca. 50 ppbv). A gap of 5 min was left prior to addition of the monoterpene to allow complete mixing. The reaction was then initiated by the addition of the monoterpene (ca. 400 ppbv for  $\alpha$ -pinene and  $\beta$ -pinene, ca. 200 ppbv for limonene), and reagent concentrations followed for roughly 30–60 min; ca. 30–90 % of the monoterpene was consumed after this time, dependent on the reaction rate with ozone. Four  $\alpha$ -pinene +  $\text{O}_3$ , five  $\beta$ -pinene +  $\text{O}_3$  and five limonene +  $\text{O}_3$  experiments were performed in total, as a function of  $[\text{H}_2\text{O}]$ . Each individual run was performed at a constant humidity, with humidity varied to cover the range of  $[\text{H}_2\text{O}] = 0.1\text{--}19 \times 10^{16} \text{ molecules cm}^{-3}$ , corresponding to an RH range of 0.1–28 % (at 298 K). Measured increases in  $[\text{SO}_2]$  agreed with measured volumetric additions across the  $\text{SO}_2$  and humidity ranges used in the experiments (Newland et al., 2015a). The experimental raw data are avail-

able at <https://doi.org/10.15124/4e9cd832-9cce-41c8-8335-c88cf32fe244> (Newland et al., 2013).

## 2.2 Analysis

A range of different SCIs are produced from the ozonolysis of each of the three monoterpenes (see Schemes 2–4), each with their own distinct chemical behaviour (i.e. yields, reaction rates); it is therefore not feasible (from these experiments) to obtain data for each SCI independently. Consequently, for analytical purposes we necessarily treat the SCI population in a simplified (lumped) manner – see Sect. 2.2.2.

SCIs are assumed to be formed in the ozonolysis reaction with a yield  $\phi$  (Reaction R1). They can then react with  $\text{SO}_2$ ,  $\text{H}_2\text{O}$ , acids formed in the ozonolysis reaction or with other species present or they can undergo unimolecular decomposition under the experimental conditions applied (Reactions R2–R5). A fraction of the SCIs produced reacts with  $\text{SO}_2$ . This fraction ( $f$ ) is the loss rate of the SCIs to  $\text{SO}_2$  ( $k_2[\text{SO}_2]$ ) compared to the sum of the total loss processes for the SCIs (Eq. 1):

$$f = \frac{k_2[\text{SO}_2]}{k_2[\text{SO}_2] + k_3[\text{H}_2\text{O}] + k_d + k_5[\text{acid}] + L}. \quad (1)$$

Here,  $L$  accounts for the sum of any other chemical loss processes for SCIs in the chamber. With the exception of reaction with acids these loss processes are expected to be negligible, as discussed later. After correction for dilution and neglecting other (non-alkene) chemical sinks for  $\text{O}_3$ , the following equation is derived. Corrections include reaction with  $\text{HO}_2$  (also produced directly during alkene ozonolysis; Alam et al., 2013; Malkin et al., 2010), which was indicated through model calculations to account for <0.5 % of ozone loss under all the experimental conditions.

$$\frac{d\text{SO}_2}{d\text{O}_3} = \phi f \quad (2)$$

From Eq. (2), regression of the loss of ozone ( $d\text{O}_3$ ) against the loss of  $\text{SO}_2$  ( $d\text{SO}_2$ ) for an experiment at a given RH determines the product  $f\phi$  at a given point in time. This quantity will vary through the experiment as  $\text{SO}_2$  is consumed and other potential SCIs co-reactants are produced, as predicted by Eq. (1). A smoothed fit was applied to the experimental data for the cumulative consumption of  $\text{SO}_2$  and  $\text{O}_3$ ,  $\Delta\text{SO}_2$  and  $\Delta\text{O}_3$ , (as shown in Fig. 2) to determine  $d\text{SO}_2/d\text{O}_3$  (and hence  $f\phi$ ) at the start of each experiment, for use in Eq. (2). The start of each experiment (i.e. when  $[\text{SO}_2] \sim 50$  ppbv) was used, as this corresponds to the greatest rate of production of the SCI and hence the largest experimental signals (i.e. greatest  $\text{O}_3$  and  $\text{SO}_2$  rate of change; greatest precision), and is the point at which the SCI +  $\text{SO}_2$  reaction has the greatest magnitude compared with any other potential loss processes for either reactant species (see discussion below).

Other potential fates for SCIs include reaction with ozone (Kjaergaard et al., 2013; Vereecken et al., 2014, 2015; Wei

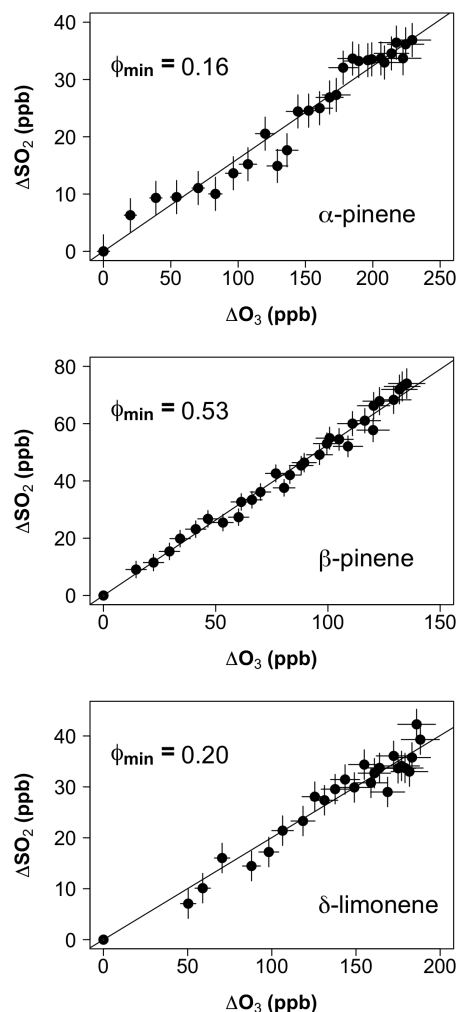


**Figure 1.**  $\Delta\text{SO}_2$  vs.  $\Delta\text{O}_3$  during excess- $\text{SO}_2$  experiments ( $[\text{H}_2\text{O}] < 5 \times 10^{15} \text{ cm}^{-3}$ ). The gradient determines the minimum SCI yield ( $\phi_{\text{min}}$ ).

et al., 2014; Chang et al., 2018), with other SCIs (Su et al., 2014; Vereecken et al., 2014), carbonyl products (Taatjes et al., 2012), acids (Welz et al., 2014) or with the parent alkene (Vereecken et al., 2014; Decker et al., 2017). Sensitivity analyses using the most recent theoretical predictions (Vereecken et al., 2015) indicate that the reaction with ozone is not significant under any of our experimental method, accounting for less than 1.5 % of SCI loss for *anti*-SCIs (based on *anti*- $\text{CH}_3\text{CHOO}$ ) at the lowest RH (worst case) experiment. Generally, SCI loss to ozone is calculated to be <1 % for all SCI. Summed losses from reaction with SCI (self-reaction), carbonyls and alkenes are likewise calculated to account for <1 % of the total SCI loss under the experimental conditions applied.

$\text{CH}_2\text{OO}$  and  $\text{CH}_3\text{CHOO}$  have been shown to react rapidly ( $k = 1\text{--}5 \times 10^{-10} \text{ cm}^3 \text{ s}^{-1}$ ) with formic and acetic acid (Welz et al., 2014). In ozonolysis experiments, Sipilä

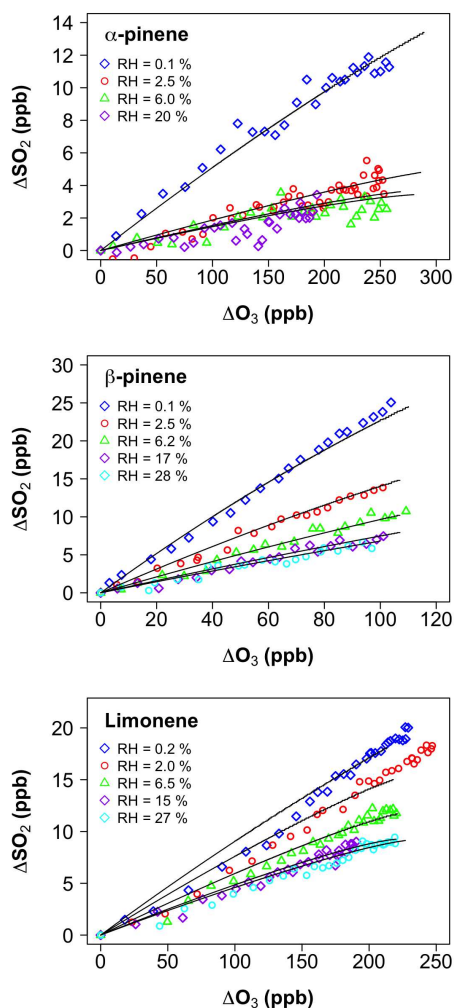


**Figure 2.** Cumulative consumption of  $\text{SO}_2$  as a function of cumulative consumption of  $\text{O}_3$  and  $\Delta\text{SO}_2$  versus  $\Delta\text{O}_3$  for the ozonolysis of  $\alpha$ -pinene,  $\beta$ -pinene and limonene in the presence of  $\text{SO}_2$  at a range of water vapour concentrations, from  $1 \times 10^{15}$  to  $1.9 \times 10^{17} \text{ cm}^{-3}$ . Symbols are experimental data, corrected for chamber dilution. Lines are smoothed fits to the experimental data.

et al. (2014) determined the relative reaction rate of acetic and formic acids with  $(\text{CH}_3)_2\text{COO}$  (i.e.  $k_5/k_2$ ) to be roughly three. Organic acid mixing ratios in this work, as measured by FTIR, reached up to a few hundred ppbv, suggesting these will likely be a significant SCI sink in our experiments. We have therefore explicitly included reaction with organic acids in our analysis, incorporating the uncertainty arising from the (unknown) acid reaction rate constant, as described in Sect. 2.2.1.

The water dimer reactions of non- $\text{CH}_2\text{OO}$  SCIs are not considered in our analysis. The effect of the water dimer reaction with  $\text{C}_{10}$  and  $\text{C}_9$  SCIs (rather than the monomer) is expected to be minor at the maximum  $[\text{H}_2\text{O}]$  ( $2 \times 10^{17} \text{ cm}^{-3}$ ) used in these experiments ( $< 30\%$  RH). Further, with analogy to the *syn-anti*- $\text{CH}_3\text{CHOO}$  system, *syn*-SCI loss to the

dimer (and monomer) will not become competitive at the highest  $[\text{H}_2\text{O}]$  used here; for *anti*-SCI, the water monomer will already be removing the majority of the SCIs at the  $[\text{H}_2\text{O}]$  at which the dimer would become a significant loss process. Hence the dimer reaction is deemed unimportant. For  $\text{CH}_2\text{OO}$ , the reaction rates with water and the water dimer have been quantified in recent EUPHORE experimental studies, and the values from Newland et al. (2015a) are used in our analysis.

Derivation of  $k(\text{SCI} + \text{H}_2\text{O})/k(\text{SCI} + \text{SO}_2)$  and  $k_d/k(\text{SCI} + \text{SO}_2)$

As noted above, a range of different SCIs are produced from the ozonolysis of the three monoterpenes (see Schemes 2–4), each with their own distinct chemical behaviour, which, treated individually, introduce too many unknowns (i.e. yields, reaction rates) for explicit analysis. Consequently for analytical purposes we treat the SCI population in a simplified (lumped) manner:

Firstly, we use the simplest model possible, assuming that a single SCI is formed in each ozonolysis reaction (Eq. 3).

$$\frac{f}{[\text{SO}_2]} = \left( [\text{SO}_2] + \frac{k_3}{k_2} [\text{H}_2\text{O}] + \frac{k_d}{k_2} + \frac{k_5}{k_2} [\text{acid}] \right)^{-1} \quad (3)$$

In a second model, for each monoterpene, the SCIs produced are assumed to belong to one of two populations, denoted SCI-A and SCI-B. These two populations are split according to the observation that the decomposition rates and reaction rates with water for the smaller SCIs ( $\text{CH}_3\text{CHOO}$ ) have been predicted theoretically (Ryzhkov and Ariya, 2004; Kuwata et al., 2010; Anglada et al., 2011) and shown experimentally (Taatjes et al., 2013; Sheps et al., 2014; Newland et al., 2015a) to exhibit a strong dependence on the structure of the molecule. The *syn*- $\text{CH}_3\text{CHOO}$  conformer, which has the terminal oxygen of the carbonyl oxide moiety in the *syn*-position to the methyl group, has been shown to react very slowly with water and to readily decompose, via the hydroperoxide mechanism, whereas the *anti*- $\text{CH}_3\text{CHOO}$  conformer, with the terminal oxygen of the carbonyl oxide moiety in the *anti*-position to the methyl group, has been shown to react fast with water and is not able to decompose via the hydroperoxide mechanism. Vereecken and Francisco (2012) have shown that all SCIs studied theoretically with an alkyl group in the *syn*-position have reaction rates with  $\text{H}_2\text{O}$  of  $k < 4 \times 10^{-17} \text{ molecule cm}^3 \text{ s}^{-1}$  (and for SCIs larger than acetone oxide,  $k < 8 \times 10^{-18} \text{ molecule cm}^3 \text{ s}^{-1}$ ).

We thus define two populations, assuming SCI-A (i.e. SCIs that exhibit chemical properties of the *anti*-type SCI) to react fast with water and not to undergo unimolecular reactions and SCI-B (i.e. SCIs that exhibit chemical properties of the *syn*-type SCI) to not react with water but to undergo unimolecular reactions. This simplification allows us to fit to the measurements using Eqs. (4) and (5), as shown below. The total SCI yields are determined by our experiments at

high SO<sub>2</sub>, and the relative yields of SCI-A and SCI-B are determined from fitting to Eq. (5). These relative yields are then compared to those predicted from the literature.

In this model,  $f = \gamma^A f^A + \gamma^B f^B$ , where  $\gamma$  is the fraction of the total SCI yield (i.e.  $\gamma^A + \gamma^B = 1$ ).  $f^A$  and  $f^B$  are the fractional losses of SCI-A and SCI-B to a reaction with SO<sub>2</sub>. Adapting Eq. (1) to include the two SCI species gives Eq. (4), where  $k_5[\text{acid}]$  accounts for the SCI + acid reaction (see discussion of reaction rate constants below).

$$f = \frac{\gamma^A k_2^A [\text{SO}_2]}{k_2^A [\text{SO}_2] + k_3 [\text{H}_2\text{O}] + k_5^A [\text{acid}]} + \frac{\gamma^B k_2^B [\text{SO}_2]}{k_2^B [\text{SO}_2] + k_d + k_5^B [\text{acid}]} \quad (4)$$

Equation (4) can be rearranged to Eq. (5) and fitted according to  $f / [\text{SO}_2]$  derived from the measurements.

$$\frac{f}{[\text{SO}_2]} = \frac{\gamma^A}{[\text{SO}_2] + \frac{k_3}{k_2^A} [\text{H}_2\text{O}] + \frac{k_5^A}{k_2^A} [\text{acid}]} + \frac{\gamma^B}{[\text{SO}_2] + \frac{k_d}{k_2^B} + \frac{k_5^B}{k_2^B} [\text{acid}]} \quad (5)$$

Using values for  $\gamma^A$  and  $\gamma^B$  from the literature and varying the assumed values of the reaction of SCIs with acid ( $k_5$ ) allows us to determine  $k_3/k_2^A$  and  $k_d/k_2^B$ .

The assumptions made here allow analysis of a very complex system. However, a key consequence is that the relative rate constants obtained from the analysis presented here are not representative of the elementary reactions of any single specific SCI isomer formed, but rather represent a quantitative ensemble description of the integrated system, under atmospheric boundary layer conditions, which may be appropriate for atmospheric modelling. Additionally our experimental approach cannot determine absolute rate constants (i.e. values of  $k_2$ ,  $k_3$ ,  $k_d$ ) in isolation and is limited to assessing their relative values, measured under atmospheric conditions, which may be placed on an absolute basis through use of an external reference value (here the SCI + SO<sub>2</sub> rate constant).

### 2.2.1 SCI yield calculation

The value for the total SCI yield of each monoterpene,  $\varphi_{\text{SCI-TOT}}$ , was determined from an experiment performed under dry conditions (RH < 1%) in the presence of excess-SO<sub>2</sub> (ca. 1000 ppbv), such that SO<sub>2</sub> scavenged the majority of the SCI. From Eq. (2), regressing  $d\text{SO}_2$  against  $d\text{O}_3$  (corrected for chamber dilution), assuming  $f$  to be unity (i.e. all the SCIs produced reacts with SO<sub>2</sub>), determines the value of  $\varphi_{\text{min}}$ , a lower limit to the SCI yield. Figure 1 shows the experimental data, from which  $\varphi_{\text{min}}$  was derived.

In reality  $f$  will be less than one at experimentally accessible SO<sub>2</sub> levels, as a fraction of the SCIs may still react with trace H<sub>2</sub>O present or undergo unimolecular reaction. The actual yield,  $\varphi_{\text{SCI}}$ , was determined by combining the result from the excess-SO<sub>2</sub> experiment with those from the series of experiments performed at lower SO<sub>2</sub>, as a function of [H<sub>2</sub>O], to obtain  $k_3/k_2$  and  $k_d/k_2$  (see Sect. 2.2.1), through an iterative process to determine the single unique value of  $\varphi_{\text{SCI}}$  which fits both data sets, as described in Newland et al. (2015a), but taking into account the proposed model in this paper of there being two SCIs produced. In this model,  $f = \gamma^A f^A + \gamma^B f^B$ . Where  $f^A = [\text{SO}_2] / ([\text{SO}_2] + k_3[\text{H}_2\text{O}] / k_2)$  and  $f^B = [\text{SO}_2] / ([\text{SO}_2] + k_d/k_2)$ , other possible SCIs sinks are assumed to be negligible. In these excess-SO<sub>2</sub> experiments,  $f^A \sim 1$  but  $f^B < 1$  since  $k_d$  still represents a significant sink.

$\gamma^A$  (and hence  $\gamma^B$ , since  $\gamma^B = 1 - \gamma^A$ ) is derived from fitting Eq. (4) to the data from the experiments performed at lower SO<sub>2</sub> for a given  $\varphi$ . Using a range of  $\varphi$  gives a range of  $\gamma$ . These different values of  $\gamma$  are used with the respective values of  $\varphi$  in fitting to Eq. (4) to determine values of  $k_3/k_2$  and  $k_d/k_2$ .

### 2.2.2 Experimental uncertainties

The uncertainty in  $k_3/k_2$  was calculated by combining the mean relative errors from the precision associated with the SO<sub>2</sub> and ozone measurements (given in Sect. 2.1) with the  $2\sigma$  error and the relative error in  $\varphi$ , using the root of the sum of the squares of these four sources of error. The uncertainty in  $k_d/k_2$  was calculated in the same way.

The uncertainty in  $\varphi_{\text{min}}$  was calculated by combining the uncertainty in  $\Delta\text{SO}_2$  and  $\Delta\text{O}_3$ , as above. The uncertainty in  $\varphi$  was calculated by applying the  $k_3/k_2$  uncertainties and combining these with the uncertainties in  $\varphi_{\text{min}}$  using the root of the sum of the squares.

## 3 Theoretical calculations

The rovibrational characteristics of all conformers of the CIs formed from  $\alpha$ -pinene and  $\beta$ -pinene, the transition states for their unimolecular reaction and their reaction with H<sub>2</sub>O were characterised quantum chemically, first using the M06-2X/cc-pVDZ level of theory, and subsequently refined at the M06-2X/aug-cc-pVTZ level. To obtain the most accurate barrier heights for reaction, it has been shown (Berndt et al., 2015; Chhantyal-Pun et al., 2017; Fang et al., 2016a, b; Long et al., 2016; Nguyen et al., 2015) that post-CCSD(T) calculations are necessary. Performing these calculations for the SCIs discussed in this paper, with up to 14 non-hydrogen atoms, is well outside our computational resources. Instead, we base our predictions on high-level CCSD(T)/aug-cc-pVTZ single-point energy calculations, performed for the reactions of nopinone oxides and the most relevant subset of

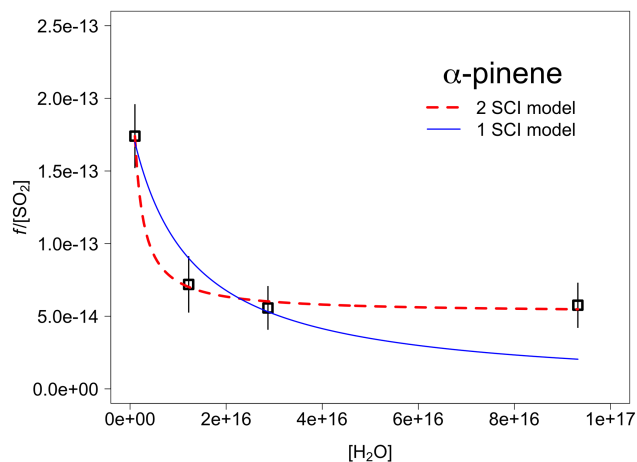


**Figure 3.** Application of a 2-SCI model fit (Eq. 4) and a single-SCI model fit (Eq. 1) to the measured values (open squares) of  $f / [\text{SO}_2]$  for  $\alpha$ -pinene. From the fit we derive relative rate constants for reaction of the  $\alpha$ -pinene-derived SCI, SCI-A and SCI-B with  $\text{H}_2\text{O}$  ( $k_3/k_2$ ) and decomposition ( $(k_d + L)/k_2$ ) assuming that  $\gamma^A = 0.40$  and  $\gamma^B = 0.60$ .

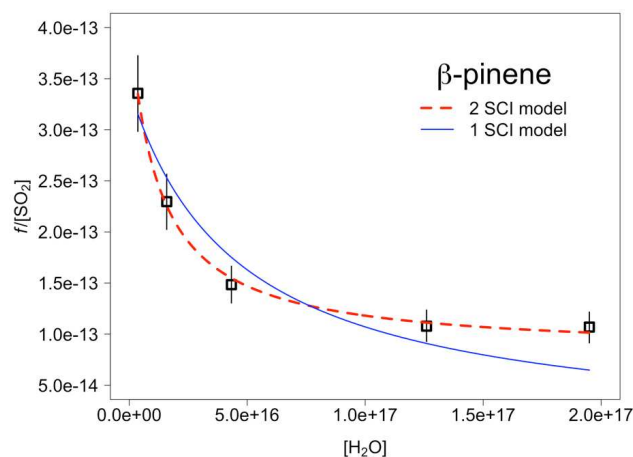


**Figure 4.** Application of a 2-SCI model fit (Eq. 4) and a single-SCI model fit (Eq. 1) to the measured values (open squares) of  $f / [\text{SO}_2]$  for  $\beta$ -pinene. From the fit we derive relative rate constants for reaction of the  $\beta$ -pinene-derived SCI, SCI-A and SCI-B with  $\text{H}_2\text{O}$  ( $k_3/k_2$ ) and decomposition ( $(k_d + L)/k_2$ ) assuming that  $\gamma^A = 0.41$  and  $\gamma^B = 0.59$ .

pinonaldehyde oxides. These data are reliable for relative rate estimates, but it remains useful to further improve the absolute barrier height predictions, as described by Vereecken et al. (2017) based on a data set with a large number of systematic calculations on smaller CIs, allowing empirical corrections to estimate the post-CCSD(T) barrier heights. Briefly, they compare rate coefficient calculations against available harmonised experimental and very high-level theoretical kinetic rate predictions and adjusts the barrier heights by 0.4 to 2.6 kcal mol<sup>-1</sup> (depending on the base methodology and the reaction type) to obtain the best agreement with these benchmark results.

Using the energetic and rovibrational data thus obtained, multi-conformer transition state theory (MC-TST) calculations (Truhlar et al., 1996; Vereecken and Peeters, 2003) were performed to obtain the rate coefficient at 298 K at the high-pressure limit. All rate predictions incorporate tunnelling corrections using an asymmetric Eckart barrier (Eckart, 1930; Johnston and Heicklen, 1962). For the reaction of CI +  $\text{H}_2\text{O}$ , a pre-reactive complex is postulated at 7 kcal mol<sup>-1</sup> below the free reactants, while the CI + ( $\text{H}_2\text{O}$ )<sub>2</sub> reaction is taken to have a pre-reactive complex of 11 kcal mol<sup>-1</sup> stability. This pre-reactive complex affects tunnelling corrections: it is assumed to always be in equilibrium with the free reactants.

In view of the high number of rotamers and the resulting computational cost, only a single limonene-derived CI isomer was studied, where the TS for the CI +  $\text{H}_2\text{O}$  reaction was analysed at the M06-2X/cc-pVDZ level of theory with only a partial conformational analysis; a limited number of the energetically most stable TS conformers thus discovered were re-optimised at the M06-2X/aug-cc-pVTZ level

of theory. These data will only be used for qualitative assessments. However, we apply the structure–activity relationships (SARs) presented by Vereecken et al. (2017) to obtain an estimate of the rate coefficients and assess the role of the individual SCI isomers in limonene ozonolysis.

All quantum chemical calculations were performed using Gaussian 09 (Frisch et al., 2010).

#### 4 GEOS-Chem model simulation

The global chemical transport model GEOS-Chem (v9-02, [www.geos-chem.org](http://www.geos-chem.org), last access: 27 April 2018, Bey et al., 2001) is used to explore the spatial and temporal variability of the atmospheric impacts of the experimentally derived chemistry. The model includes HOx–NOx–VOC–O<sub>3</sub>–BrOx chemistry (Mao et al., 2010; Parrilla et al., 2012) and a mass-based aerosol scheme. Biogenic monoterpene emissions are taken from the Model of Emissions of Gases and Aerosols from Nature (MEGAN) v2.1 inventory (Guenther et al., 2006, 2012). Transport is driven by assimilated meteorology (GEOS-5) from NASA's Global Modelling and Assimilation Office (GMAO). The model is run at 4° × 5° resolution, with the second year (2005) used for analysis and first year discarded as spin-up. The model code used for these runs is available at <https://doi.org/10.5281/zenodo.1220385> and the model run directory at <https://doi.org/10.5281/zenodo.1220387> (GEOS-Chem team v9-02, 2018).

In this study, the standard simulation was expanded to include emissions of seven monoterpene species ( $\alpha$ -pinene,  $\beta$ -pinene, limonene, myrcene, ocimene, carene and sabinene) from MEGAN v2.1. The ozonolysis scheme for

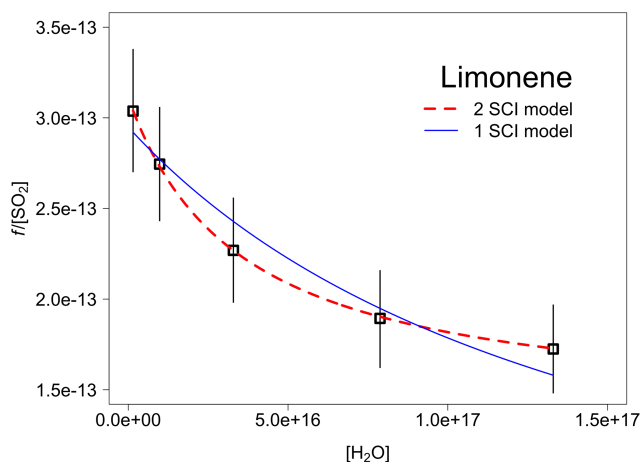


**Figure 5.** Application of a 2-SCI model fit (Eq. 4) and a single-SCI model fit (Eq. 1) to the measured values (open squares) of  $f / [\text{SO}_2]$  for limonene. From the fit we derive relative rate constants for reaction of the limonene-derived SCI, SCI-A and SCI-B with  $\text{H}_2\text{O}$  ( $k_3/k_2$ ) and decomposition ( $(k_d + L)/k_2$ ) assuming that  $\gamma^A = 0.22$  and  $\gamma^B = 0.78$ .

each monoterpene, detailed in Sect. 7.1, considers the formation of one or two types of SCI and their subsequent reaction with  $\text{SO}_2$ ,  $\text{H}_2\text{O}$  or unimolecular decomposition. The reaction rates of the monoterpenes with  $\text{OH}$ ,  $\text{O}_3$  and  $\text{NO}_3$  are detailed in Supplement Table S1.

## 5 Experimental results

### 5.1 SCI yield

Figure 1 shows the lower limit to the SCI yield,  $\varphi_{\min}$ , for the three monoterpenes, determined from fitting Eq. (5) to the experimental data. This gives values of  $0.16 (\pm 0.01)$  for  $\alpha$ -pinene,  $0.53 (\pm 0.01)$  for  $\beta$ -pinene and  $0.20 (\pm 0.01)$  for limonene. These  $\varphi_{\min}$  values were then corrected as described in Sect. 2.2.2 using the  $k_3/k_2$  and  $k_d/k_2$  values determined from the measurements shown in Figs. 3–5 using Eq. (4). The corrected yields,  $\varphi_{\text{SCI}}$ , are  $0.19 (\pm 0.01)$  for  $\alpha$ -pinene,  $0.60 (\pm 0.03)$  for  $\beta$ -pinene and  $0.23 (\pm 0.01)$  for limonene. Uncertainties are  $\pm 2\sigma$  and represent the combined systematic (estimated measurement uncertainty) and precision components. Literature yields for SCI production from monoterpene ozonolysis are summarised in Table 1.

The value derived for the total SCI yield from  $\alpha$ -pinene in this work of 0.19 agrees within the uncertainties, with a value of  $0.15 (\pm 0.07)$  reported by Sipilä et al. (2014) and a value of 0.20 applied in the MCMv3.3.1.

The total SCI yield from  $\beta$ -pinene derived in this work, 0.60, agrees reasonably well with the recent experimental work of Ahrens et al. (2014), who derived a total SCI yield of 0.50 (0.40 for the sum of CI-1 and CI-2 and 0.10 for  $\text{CH}_2\text{OO}$ , which is assumed to be formed almost completely

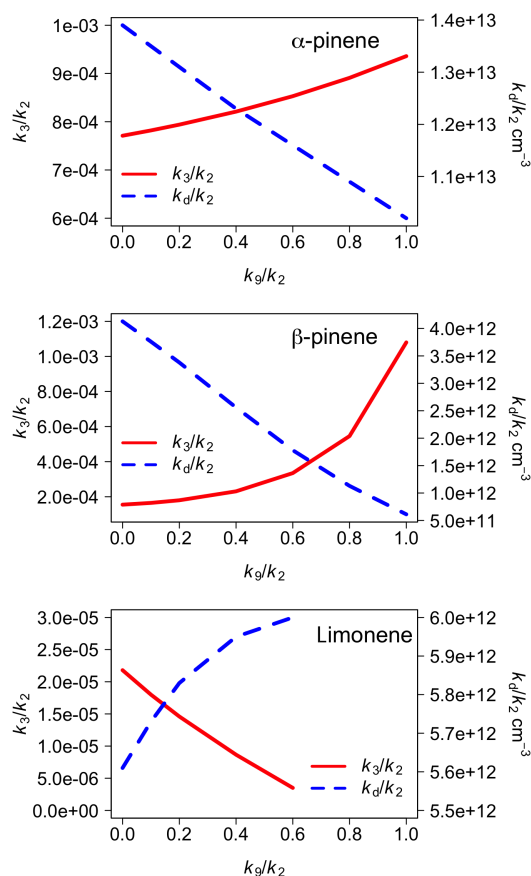


**Figure 6.** Variation of  $k_3/k_2$  ( $k(\text{SCI-A} + \text{H}_2\text{O}) / (k(\text{SCI-A} + \text{SO}_2))$ ) and  $k_d$  ( $k(\text{SCI-B unimol.}) / (k(\text{SCI-B} + \text{SO}_2))$ ) as a function of the ratio  $k_3/k_2$  ( $k(\text{SCI} + \text{acid}) / k(\text{SCI} + \text{SO}_2)$ ), derived from least squares fit of Eq. (4) to measurements shown in Figs. 3–5 for  $\alpha$ -pinene,  $\beta$ -pinene and limonene respectively.

stabilised). The MCMv3.3.1 applies a total SCI yield of 0.25, of which 0.10 is a C9-CI and 0.15 is  $\text{CH}_2\text{OO}$ . Earlier studies also tended to derive lower total SCI yields ranging from 0.25 to 0.27 (Hasson et al., 2001; Hatakeyama et al., 1984).

The total SCI yield from limonene derived in this work,  $0.23 (\pm 0.01)$  agrees with the recently determined yield from Sipilä et al. (2014) of  $0.27 (\pm 0.12)$ . Leungsakul et al. (2005) derived a somewhat higher yield of 0.34, while the MCMv3.3.1 applies a lower yield of 0.135.

### 5.2 $k_3(\text{SCI} + \text{H}_2\text{O}) / k_2(\text{SCI} + \text{SO}_2)$ and $k_d/k_2(\text{SCI} + \text{SO}_2)$ analysis

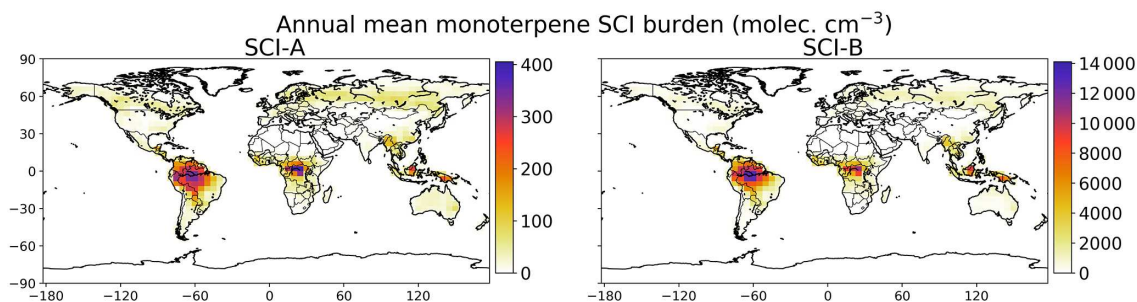
Figure 2 shows the loss of  $\text{SO}_2$  as ozone is consumed by reaction with the monoterpene for each of the three systems. Box modelling results suggest that  $>99\%$  of this  $\text{SO}_2$  removal is caused by reaction with SCIs produced in the alkene–ozone reaction (rather than e.g. reaction with  $\text{OH}$ , which is scavenged by cyclohexane). When the experiments are repeated at higher relative humidity, the rate of loss of  $\text{SO}_2$  decreases.

**Table 1.** Monoterpene SCI yields derived in this work and reported in the literature.

$\varphi_{\text{SCI}}$	Reference	Notes	Methodology
<b><math>\alpha</math>-pinene</b>			
0.19 ( $\pm 0.01$ )	This work		SO <sub>2</sub> loss
0.15 ( $\pm 0.07$ )	Sipilä et al. (2014)		Formation of H <sub>2</sub> SO <sub>4</sub>
0.22	Taipale et al. (2014)		
0.125 ( $\pm 0.04$ )	Hatakeyama et al. (1984)		Formation of H <sub>2</sub> SO <sub>4</sub>
0.20	MCMv3.3.1 <sup>a</sup>		
<b><math>\beta</math>-pinene</b>			
0.60 ( $\pm 0.03$ )	This work		SO <sub>2</sub> loss
0.46	Ahrens et al. (2014)	$\varphi_{\text{C9-SCI}}$ : 0.36 $\varphi_{\text{CH2OO}}$ : 0.10	FTIR detection
0.25	MCMv3.3.1 <sup>a</sup>	$\varphi_{\text{C9-SCI}}$ : 0.102 $\varphi_{\text{CH2OO}}$ : 0.148	
0.42	Nguyen et al. (2009a)	$\varphi_{\text{C9-SCI}}$ : 0.37 $\varphi_{\text{CH2OO}}$ : 0.05	Theoretical
0.51	Winterhalter et al. (2000)	$\varphi_{\text{C9-SCI}}$ : 0.35 $\varphi_{\text{CH2OO}}$ : 0.16	Change in nopinone yields $f([\text{H}_2\text{O}])$
0.44	Kotzias et al. (1990)		Formation of H <sub>2</sub> SO <sub>4</sub>
0.25	Hatakeyama et al. (1984)		Formation of H <sub>2</sub> SO <sub>4</sub>
0.30	Zhang and Zhang (2005)	$\varphi_{\text{C9-SCI}}$ : 0.22 $\varphi_{\text{CH2OO}}$ : 0.08	
> 0.27	Ma and Marston (2008)	$\varphi_{\text{C9-SCI}}$ : 0.27 $\varphi_{\text{CH2OO}}$ : 0.16 <sup>a</sup> $\varphi_{\text{CH2OO}}$ : 0.06 <sup>b</sup>	Change in nopinone yields $f([\text{H}_2\text{O}])$
0.27	Hasson et al. (2001)		Change in nopinone yields $f([\text{H}_2\text{O}])$
<b>Limonene</b>			
0.23 ( $\pm 0.01$ )	This work		SO <sub>2</sub> loss
0.27 ( $\pm 0.12$ )	Sipilä et al. (2014)		Formation of H <sub>2</sub> SO <sub>4</sub>
0.34	Leungsakul et al. (2005)	$\varphi_{\text{C10-SCI}}$ : 0.26 $\varphi_{\text{CI-x}}$ : 0.04 $\varphi_{\text{CH2OO}}$ : 0.05	Measurement of stable particle and gas-phase products
0.135	MCMv3.3.1 <sup>a</sup>		

Uncertainty ranges ( $\pm 2\sigma$ , parentheses) indicate combined precision and systematic measurement error components for this work and are given as stated for literature studies. All referenced experimental studies produced SCIs from MT + O<sub>3</sub> and were conducted between 700 and 760 Torr.

<sup>a</sup> <http://mcm.leeds.ac.uk/MCM/> (last access: 27 April 2018) (Jenkin et al., 2015). <sup>a</sup> Assuming 100 % stabilisation. <sup>b</sup> Assuming 40 % stabilisation.

**Figure 7.** Annual mean monoterpene SCI-A and SCI-B concentrations ( $\text{cm}^{-3}$ ) in the surface layer of the GEOS-Chem simulation.

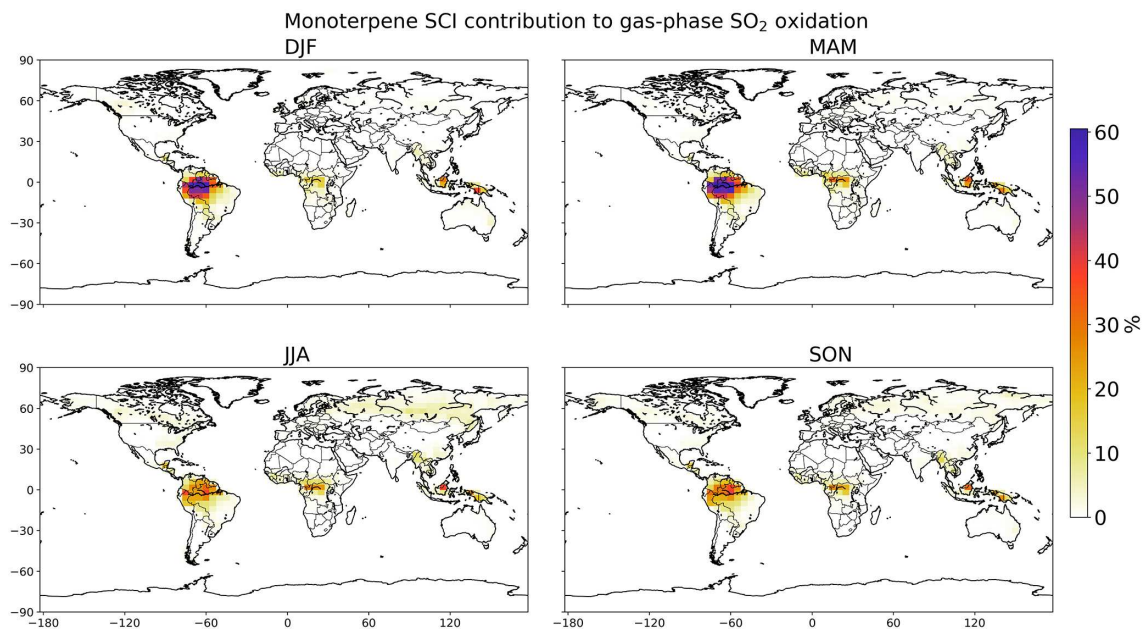


**Figure 8.** Seasonal SO<sub>2</sub> oxidation by monoterpene SCIs as percentage of total gas-phase SO<sub>2</sub> oxidation in the surface layer.

This is as expected from Eq. (1) and suggests that there is competition between SO<sub>2</sub> and H<sub>2</sub>O for reaction with the SCIs produced, in agreement with observations of smaller SCI, which demonstrate the same competition under atmospherically relevant conditions (Newland et al., 2015a, b).

However, as the relative humidity is increased further, the SO<sub>2</sub> loss does not fall to (near) zero as would be expected from Eq. (1). This suggests that at high [H<sub>2</sub>O] the amount of SO<sub>2</sub> loss becomes less sensitive to [H<sub>2</sub>O]. This is most likely due to there being at least two chemically distinct SCI species present. This behaviour was previously observed for CH<sub>3</sub>CHO by Newland et al. (2015a) and fits with the current understanding that the reactivity of SCIs is structure dependent.

To recap Sect. 2.2.1, the analysis presented here considers two models to fit the observations. The first of these (Eq. 3) assumes the formation of a single SCI species, which, in addition to reacting with SO<sub>2</sub>, can react with water, undergo unimolecular reaction or react with acid. It is clearly evident from Figs. 3–5 that this model does not give a good fit to the observations for any of the monoterpene systems studied. Therefore, the results of this (single SCI) approach are not discussed explicitly hereafter. The second of the models (Eq. E5) assumes the formation of two lumped, chemically distinct populations of SCI, denoted SCI-A and SCI-B. SCI-A is assumed to react fast with H<sub>2</sub>O and to have minimal decomposition. Conversely, SCI-B is assumed to have a negligible reaction with water under the experimental conditions applied but to undergo rearrangement via a VHP. We use a least squares fit of Eq. (5) to the data to determine the values of  $k_3/k_2$  and  $k_d/k_2$ . This approach fits the data well

(Figs. 3–5) for all 3 monoterpenes and represents the overall attributes of the SCIs that formed but as noted, does not represent an explicit determination of individual conformer-dependent rate constants.

### 5.2.1 $\alpha$ -pinene

The  $\alpha$ -pinene system is sensitive to water vapour at the low H<sub>2</sub>O range, with the SO<sub>2</sub> loss falling dramatically when the RH is increased from 0.1 to 2.5 % (Fig. 2). However, at higher RH the SO<sub>2</sub> loss appears to be rather insensitive to [H<sub>2</sub>O].

CI-1 can be formed in either a *syn*- (1a) or *anti*-configuration (1b), whereas both CI-2 conformers are in a *syn*-configuration (see Scheme 2). For one of the two conformers of CI-2 (CI-2b), the hydrogen atom available for abstraction by the terminal oxygen of the carbonyl oxide group is attached to the carbon on the 4-membered ring. This has been shown in the  $\beta$ -pinene system to make a large difference with respect to the ability of the hydrogen to be abstracted and to undergo the VHP mechanism (Rickard et al., 1999; Nguyen et al., 2009a). This therefore suggests that CI-2b may exhibit characteristics of both SCI-A and SCI-B. Ma et al. (2008) infer a probable equal yield of the two basic CI structures. This would suggest a relative yield for SCI-A of 0.25–0.50 (depending on the precise nature of CI-2b). Fitting Eq. (4) to the data and allowing  $\lambda$  to vary determines values of  $\gamma^A = 0.40$  and  $\gamma^B = 0.60$  (Fig. 3).

In Fig. 3, Eq. (4) is fitted to the  $\alpha$ -pinene measurements, assuming  $k(\text{SCI} + \text{acid}) / k(\text{SCI} + \text{SO}_2) = 0$ . This derives a minimum value for  $k(\text{SCI-A} + \text{H}_2\text{O}) / k(\text{SCI-A} + \text{SO}_2)$ , the water-dependent fraction of the SCI and a maximum value

for  $k$  (decomposition: SCI-B) /  $k(\text{SCI-B} + \text{SO}_2)$ , the water independent fraction of the SCI. The kinetic parameters derived from the fitting are displayed in Table 2.

Figure 6 shows the variation in the derived  $k_3/k_2$  and  $k_d/k_2$  values as the ratio  $k_5/k_2$ ,  $k(\text{SCI} + \text{acid}) / k(\text{SCI} + \text{SO}_2)$ , which is varied from zero to one. The derived  $k_3/k_2$  increases by about 40 % from  $1.4 (\pm 0.34) \times 10^{-3}$  to  $2.0 (\pm 0.49) \times 10^{-3}$ . The derived  $k_d/k_2$  value decreases again by about 40 % from  $8.2 (\pm 1.5) \times 10^{12} \text{ cm}^{-3}$  to  $5.1 (\pm 0.93) \times 10^{12} \text{ cm}^{-3}$ .

The derived limits to the relative rate constants can be put on an absolute scale using the  $k(\text{SCI} + \text{SO}_2)$  values for  $\text{CH}_3\text{CHO}$  from Sheps et al. (2014) for the *syn*- and *anti*-conformers. For *syn* this is  $2.9 \times 10^{-11} \text{ cm}^3 \text{ s}^{-1}$  and for *anti* this is  $2.2 \times 10^{-10} \text{ cm}^3 \text{ s}^{-1}$ . The *syn*-rate constant is applied to the derived  $k(\text{decomposition:SCI-B}) / k(\text{SCI-B} + \text{SO}_2)$  value and the *anti* rate constant to the  $k(\text{SCI-A} + \text{H}_2\text{O}) / k(\text{SCI-A} + \text{SO}_2)$  value. It should be noted that the  $k_2$  values are for quite different SCIs to those formed in this study and to our knowledge no structure-specific  $k(\text{SCI} + \text{SO}_2)$  have been reported for monoterpene-derived SCI, though Ahrens et al. (2014) determine an average  $k_2 \sim 4 \times 10^{-11} \text{ cm}^3 \text{ s}^{-1}$  for SCI derived from  $\beta$ -pinene, i.e. a value within an order of magnitude of those determined for the smaller SCIs  $\text{CH}_2\text{OO}$ ,  $\text{CH}_3\text{CHO}$  and  $(\text{CH}_3)_2\text{COO}$  (e.g. Welz et al., 2012; Taatjes et al., 2013; Sheps et al., 2014; Huang et al., 2015). Using the Sheps et al. (2014) values yields  $k(\text{SCI-A} + \text{H}_2\text{O}) > 3.1 (\pm 0.75) \times 10^{-13} \text{ cm}^3 \text{ s}^{-1}$  and  $k(\text{decomposition:SCI-B}) < 240 (\pm 44) \text{ s}^{-1}$  (using the values derived for  $k(\text{SCI-A} + \text{acid}) / k(\text{SCI-A} + \text{SO}_2) = 0$ ). This  $k_3$  value is an order of magnitude larger than the rate constants determined for the smaller *anti*- $\text{CH}_3\text{CHO}$  in the direct studies of Sheps et al. (2014) ( $2.4 \times 10^{-14} \text{ cm}^3 \text{ s}^{-1}$ ) and Taatjes et al. (2013) ( $1.0 \times 10^{-14} \text{ cm}^3 \text{ s}^{-1}$ ). The decomposition value derived for SCI-B is of the same order of magnitude as that for *syn*- $\text{CH}_3\text{CHO}$  ( $348 \pm 332 \text{ s}^{-1}$ ) and  $(\text{CH}_3)_2\text{COO}$  ( $819 \pm 190 \text{ s}^{-1}$ ) from Newland et al. (2015a) (using updated direct measurement values of  $k_2$  from Sheps et al. (2014) and Huang et al. (2015) for *syn*- $\text{CH}_3\text{CHO}$  and  $(\text{CH}_3)_2\text{COO}$  respectively) and within the range from the recent paper by Smith et al. (2016) which derives a decomposition rate for  $(\text{CH}_3)_2\text{COO}$  of  $269 (\pm 82) \text{ s}^{-1}$  at 283 K increasing to  $916 (\pm 56) \text{ s}^{-1}$  at 323 K.

Sipilä et al. (2014) applied a single-SCI analysis approach to the formation of  $\text{H}_2\text{SO}_4$  from  $\text{SO}_2$  oxidation in the presence of the  $\alpha$ -pinene ozonolysis system. They determined that for  $\alpha$ -pinene,  $k_d \gg k(\text{SCI} + \text{H}_2\text{O})[\text{H}_2\text{O}]$  for  $[\text{H}_2\text{O}] < 2.9 \times 10^{17} \text{ cm}^{-3}$ , i.e. that the fate of SCIs formed in the system is rather insensitive to  $[\text{H}_2\text{O}]$ . Across the  $[\text{SO}_2]$  and RH ranges used in their study, the results obtained here would indicate  $\text{H}_2\text{O}$  to always be the dominant sink for SCI-A; i.e. the fact that Sipilä et al. (2014) see similar  $\text{H}_2\text{SO}_4$  production across the RH range in their study is consistent with these results.

### 5.2.2 $\beta$ -pinene

Two recent studies (Nguyen et al., 2009a; Ahrens et al., 2014) have suggested yields of the two  $\text{C}_9$ -CI (CI-3 and CI-4; see Scheme 3) obtained from  $\beta$ -pinene ozonolysis to be roughly equal. In these studies Ahrens et al. (2014) assume a  $\text{CH}_2\text{OO}$  yield of 0.10 while Nguyen et al. (2009a) determine theoretically the yield of  $\text{CH}_2\text{OO}$  to be 0.05. Another theoretical study (Zhang and Zhang, 2005) predicted a  $\text{CH}_2\text{OO}$  yield of 0.08. In experimental studies, Winterhalter et al. (2000) determined the  $\text{CH}_2\text{OO}$  yield to be  $0.16 (\pm 0.04)$  from measuring the nopinone yield and assuming it to be entirely a primary ozonolysis product (i.e. the co-product of  $\text{CH}_2\text{OO}$  formation) and Ma and Marston (2008) determine a summed contribution of 84 % ( $\pm 0.03$ ) for the two  $\text{C}_9$ -CI (i.e. a 16 %  $\text{CH}_2\text{OO}$  yield). The theoretical studies are somewhat lower than the experimental but Nguyen et al. (2009a) note that CI-4 is likely to form additional nopinone in bimolecular reactions. The  $\text{CH}_2\text{OO}$  is assumed to all be formed stabilised (e.g. Nguyen et al., 2009a).

SCI-3 is expected to undergo unimolecular reactions at least an order of magnitude faster than SCI-4 (Nguyen et al., 2009a; Ahrens et al., 2014). The reaction of SCI-3 with water is expected to be slow based on the calculations presented in Table 4, with a pseudo first order reaction rate of  $0.3 \text{ s}^{-1}$  at the highest  $[\text{H}_2\text{O}]$  used here,  $2 \times 10^{17} \text{ cm}^{-3}$ , 298 K, whereas the water reaction with SCI-4 is expected to be considerably faster with a pseudo first order reaction rate of  $85 \text{ s}^{-1}$  at  $[\text{H}_2\text{O}] = 2 \times 10^{17} \text{ cm}^{-3}$ , 298 K. This reaction would thus be expected to be competitive with reaction with  $\text{SO}_2$  for SCI-4 under the experimental conditions employed. This is in agreement with the observations of Ma and Marston (2008), which show a clear dependence of nopinone formation on RH (presumed to be formed from  $\text{SCI} + \text{H}_2\text{O}$ ). Fitting Eq. (4) to the data determines values of  $\gamma^A = 0.41$  and  $\gamma^B = 0.59$  (Fig. 4).

Using these values, and assuming  $k(\text{SCI} + \text{acid}) / k(\text{SCI} + \text{SO}_2) = 0$ , yields a  $k(\text{SCI-A} + \text{H}_2\text{O}) / k(\text{SCI-A} + \text{SO}_2)$  value of  $> 1.0 (\pm 0.27) \times 10^{-4}$  and a  $k(\text{decomposition:SCI-B}) / k(\text{SCI-B} + \text{SO}_2)$  value of  $< 6.0 (\pm 1.3) \times 10^{12} \text{ cm}^{-3}$  (Table 2).

As shown in Fig. 6, increasing  $k_5/k_2$ ,  $k(\text{SCI} + \text{acid}) / k(\text{SCI} + \text{SO}_2)$ , from zero to one, decreases the derived  $k_d/k_2$  from  $6.0 (\pm 1.3) \times 10^{12} \text{ cm}^{-3}$  to  $1.8 (\pm 0.39) \times 10^{12} \text{ cm}^{-3}$ . The derived  $k_3/k_2$  increases by a factor of 4 from  $1.0 (\pm 0.27) \times 10^{-4}$  to  $3.7 (\pm 1.0) \times 10^{-4}$ .

These values can be put on an absolute scale (using the values derived above for  $k_5/k_2 = 0$ ). For SCI-A,  $k(\text{SCI} + \text{SO}_2)$  is taken as the experimentally determined value of  $4 \times 10^{-11} \text{ cm}^3 \text{ s}^{-1}$  from Ahrens et al. (2014). For SCI-B, the *syn*- $\text{CH}_3\text{CHO}$   $k(\text{SCI} + \text{SO}_2)$  value determined by Sheps et al. (2014) is used. This gives values of  $k(\text{SCI-A} + \text{H}_2\text{O}) > 4 \times 10^{-15} (\pm 1) \text{ cm}^3 \text{ s}^{-1}$  and  $k(\text{decomposition:SCI-B}) < 170 (\pm 38) \text{ s}^{-1}$ .

**Table 2.** Monoterpene-derived SCI relative and absolute<sup>a</sup> rate constants derived in this work.

SCI	$10^5 k_3/k_2$	$10^{15} k_3$ (cm <sup>3</sup> s <sup>-1</sup> )	$10^{-12} k_d/k_2$ (cm <sup>-3</sup> )	$k_d$ (s <sup>-1</sup> )
<i>α</i> -pinene				
SCI-A	> 140 (±34)	> 310 (±75) <sup>a</sup>		
SCI-B			< 8.2 (±1.5)	< 240 (±44) <sup>c</sup>
<i>β</i> -pinene				
SCI-A	> 10 (±2.7)	> 4 (±1) <sup>b</sup>		
SCI-B			< 6.0 (±1.3)	< 170 (±38) <sup>c</sup>
Limonene				
SCI-A	< 3.5 (± 0.2)	< 7.7 (±0.6) <sup>a</sup>		
SCI-B			> 4.5 (±0.1)	> 130 (±3) <sup>c</sup>

Uncertainty ranges ( $\pm 2\sigma$ , parentheses) indicate combined precision and systematic measurement error components. <sup>a</sup> Scaled to an absolute value using  $k_2(\text{anti-CH}_3\text{CHOO}) = 2.2 \times 10^{-10} \text{ cm}^3 \text{ s}^{-1}$  (Sheps et al., 2014). <sup>b</sup> Scaled to an absolute value using  $k_2(\text{anti-CH}_3\text{CHOO}) = 4 \times 10^{-11} \text{ cm}^3 \text{ s}^{-1}$  (Ahrens et al., 2014). <sup>c</sup> Scaled using  $k_2(\text{syn-CH}_3\text{CHOO}) = 2.9 \times 10^{-11} \text{ cm}^3 \text{ s}^{-1}$  (Sheps et al., 2014).

### 5.2.3 Limonene

For the limonene measurements presented in Fig. 2,  $(d\text{SO}_2/d\text{O}_3)/dt$  appears to be non-linear, with a jump in  $d\text{SO}_2/d\text{O}_3$  between 120 and 150 ppbv of ozone consumed. This is most evident in the two lowest RH runs (0.2 and 2.0 %). Limonene is the fastest reacting of the systems presented here, with the alkene reaction having consumed 100 ppbv of ozone within the first 5 min. The limonene sample required about 5 min of heating before the entire sample was volatilised and injected into the chamber. This therefore may account for the apparent non-linear nature of  $d\text{SO}_2/d\text{O}_3$  in Fig. 2.

The  $\text{SO}_2$  loss in the limonene–ozone system is less affected by increasing  $\text{H}_2\text{O}$  than for either  $\alpha$  or  $\beta$ -pinene (Fig. 5), with the values of  $f/[\text{SO}_2]$  ( $y$  axis) varying by roughly a factor of 2 over the RH range applied compared to more than a factor of 3 for the other two systems. Hence it might be expected that there is little formation of  $\text{H}_2\text{O}$ -dependent SCI or that it has a rather slow reaction rate with water.

Fitting Eq. (4) to the data determines values of  $\gamma^A = 0.22$  and  $\gamma^B = 0.78$  (Fig. 5). This is broadly in line with the ratio recommended in the MCMv3.3.1 of 0.27 : 0.73 and with that proposed in Leungsakul et al. (2005), who use a CI-A : CI-B ratio of 0.35 : 0.65, but also include some stabilisation of  $\text{CH}_2\text{OO}$  and  $\text{C}_9\text{-CI}$  from ozone reaction at the exocyclic bond. This yields a  $k(\text{SCI-A} + \text{H}_2\text{O})/k(\text{SCI-A} + \text{SO}_2)$  value of  $< 3.5 (\pm 0.20) \times 10^{-5}$  and a  $k(\text{decomposition:SCI-B})/k(\text{SCI-B} + \text{SO}_2)$  value of  $> 4.5 (\pm 0.10) \times 10^{12} \text{ cm}^{-3}$ .

Figure 6 shows that the derived  $k_d/k_2$  increases by about 7 % as  $k(\text{SCI} + \text{acid})/k(\text{SCI} + \text{SO}_2)$  ranges from 0.0 to 0.8. The derived  $k_3/k_2$  becomes negative at  $k(\text{SCI} + \text{acid})/k(\text{SCI} + \text{SO}_2) > 0.8$ , placing an upper limit on this ratio, i.e.  $k_5/k_2 < 0.8$ , for the limonene system.

Placing these values on an absolute scale (using the values derived for  $k_5/k_2 = 0$ ), using the  $\text{CH}_3\text{CHOO}$  *syn*- and *anti*- $k(\text{SCI} + \text{SO}_2)$  determined by Sheps et al. (2014), yields values of  $< 7.7 (\pm 0.60) \times 10^{-15} \text{ cm}^3 \text{ s}^{-1}$  and  $> 130 (\pm 3) \text{ s}^{-1}$  for  $k_3$  and  $k_d$  respectively. These values are similar to those derived for the SCI-A and SCI-B formed from  $\beta$ -pinene. The  $k_3$  value is a factor of 3 smaller than that determined by Sheps et al. (2014) for  $k_3(\text{anti-CH}_3\text{CHOO} + \text{H}_2\text{O})$ ,  $2.4 \times 10^{-14} \text{ cm}^3 \text{ s}^{-1}$ .

Sipilä et al. (2014) applied a single-SCI analysis approach to the formation of  $\text{H}_2\text{SO}_4$  from  $\text{SO}_2$  oxidation by the limonene ozonolysis system and determined that, similarly to  $\alpha$ -pinene,  $k(\text{decomp.}) \gg k(\text{SCI} + \text{H}_2\text{O})[\text{H}_2\text{O}]$  for  $[\text{H}_2\text{O}] < 2.9 \times 10^{17} \text{ cm}^{-3}$ ; i.e. the system is rather insensitive to  $[\text{H}_2\text{O}]$ . Our data are consistent with the limonene system being less sensitive to  $[\text{H}_2\text{O}]$  than the SCI populations derived from the other two monoterpenes reported here.

### 5.2.4 Experimental summary

The reaction rates of SCI-A (i.e. SCIs that exhibit chemical properties of the *anti*-type SCI) derived from the three different monoterpenes with a water range from  $< 0.8$  to  $> 31 \times 10^{-14} \text{ cm}^3 \text{ s}^{-1}$  are broadly in line with the derived rates of Sheps et al. (2014) for *anti-CH}\_3\text{CHOO} of  $2.4 \times 10^{-14} \text{ cm}^3 \text{ s}^{-1}$ . The decomposition rates of SCI-B (i.e. SCIs that exhibit chemical properties of the *syn*-type SCI) are of the order of 100–250  $\text{s}^{-1}$ . This is in line with those derived for *syn-CH}\_3\text{CHOO} + \text{SO}\_2 from *cis*- and *trans*-but-2-ene ozonolysis and  $(\text{CH}_3)_2\text{COO}$  by Newland et al. (2015a) of  $348 (\pm 332) \text{ s}^{-1}$  and  $819 (\pm 190) \text{ s}^{-1}$  respectively (assuming  $k(\text{syn-CH}_3\text{CHOO} + \text{SO}_2) = 2.9 \times 10^{-11} \text{ cm}^3 \text{ s}^{-1}$  (Sheps et al., 2014) and  $k((\text{CH}_3)_2\text{COO} + \text{SO}_2) = 2.9 \times 10^{-10} \text{ cm}^3 \text{ s}^{-1}$ ; Huang et al., 2015) and recent results from Smith et**

**Table 3.** Unimolecular reactions for the CIs derived from  $\alpha$ -pinene,  $\beta$ -pinene and  $d$ -limonene, as derived by Vereecken et al. (2017). Barrier heights (kcal mol<sup>-1</sup>) listed estimated post-CCSD(T) energies.

Carbonyl oxide	Reaction	$E_b$	$k(298\text{ K})/\text{s}^{-1}$
$\alpha$ -pinene			
CI-1a	1,4-H migration	15.8	600
	SOZ-formation	15.6	$5 \times 10^{-2}$
	1,3-ring closure	21.6	$1 \times 10^{-3}$
CI-1b	1,3-ring closure	14.8	60
	1,3-H migration	29.0	$1 \times 10^{-6}$
CI-2a	1,4-H migration	16.3	250
	1,3-ring closure	20.8	$6 \times 10^{-3}$
CI-2b	1,4-H migration	17.0	60
	SOZ-formation	13.5	8
	Ring closure	19.9	$3 \times 10^{-2}$
$\beta$ -pinene			
CI-3	1,4-H migration	15.7	375
	1,3-ring closure	21.1	$2 \times 10^{-3}$
CI-4	1,3-ring closure	17.2	2.0
	Ring opening	23.6	(Slow, Nguyen et al., 2009a)
	1,4-H migration	24.9	(Slow, Nguyen et al., 2009a)
CH <sub>2</sub> OO	1,3-ring closure	19.0	0.3
	1,3-H migration	30.7	$1 \times 10^{-7}$
Limonene*			
CI-5a	1,4-H migration	SAR	200*
CI-5b	1,3-ring closure	SAR	75*
CI-6a	1,4-H migration	SAR	430*
CI-6b	1,4-H migration	SAR	700*
CI-7a	1,4-H migration	SAR	15
CI-7b	1,4-H migration	SAR	600

\* Formation of secondary ozonides (SOZ) is not included and could be the dominant unimolecular loss.

al. (2016) of  $269\text{--}916\text{ s}^{-1}$  (strongly dependent on temperature) for  $(\text{CH}_3)_2\text{COO}$  decomposition. In this work we only derive relative rates, but the similarity of the  $k_3$  and  $k_d$  values derived when the  $k_2$  values for *syn*- and *anti*- $\text{CH}_3\text{CHOO}$  from Sheps et al. (2014) are applied is consistent with the recent work of Ahrens et al. (2014), suggesting that large SCI, derived from monoterpenes, demonstrate a similar reactivity towards  $\text{SO}_2$  to that of smaller SCI. One uncertainty in the derivation of the kinetics presented herein is the reactions of the SCIs produced with organic acids. These acids were present in the experiments (owing to formation in the monoterpene ozonolysis reactions themselves) at levels which may have been a competitive sink for the SCI.

## 6 Theoretical results and comparison to experiments

The theoretically predicted rate coefficients for unimolecular reactions of the monoterpene SCIs are listed in Table 3, while those for the reaction with  $\text{H}_2\text{O}$  are listed in Table 4. These

data can be compared with the experimental data obtained in this work.

### 6.1 $\alpha$ -pinene

The theory-based rate coefficients show one pinonaldehyde oxide, CI-1b, with a rate of reaction with water that is significantly faster than the remaining  $\alpha$ -pinene-derived CIs. Comparing this rate to the experimental data shows that CI-1b corresponds to SCI-A, with matching rate coefficients within an order of magnitude, i.e. within the expected uncertainty. We thus deduce that SCI-A is CI-1b. The remaining pinonaldehyde oxides, CI-1a, CI-2a and CI-2b, react predominantly through unimolecular reactions, in which theory-based rate coefficients range from 60 to  $600\text{ s}^{-1}$ . All are within a factor of 4 of the experimentally derived population-averaged rate of  $240 \pm 44\text{ s}^{-1}$ , i.e. matching within the uncertainty margins. The unimolecular rate coefficients of this set of CIs are sufficiently close that it is not feasible to separate these in the experimental data, so we can only conclude that SCI-B in the

**Table 4.** Rate coefficients ( $\text{cm}^3 \text{ molecule}^{-1} \text{ s}^{-1}$ ) for the reaction of CIs with  $\text{H}_2\text{O}$  and  $(\text{H}_2\text{O})_2$  as predicted by Vereecken et al. (2017). Values are based on explicit CCSD(T)/aug-cc-pVTZ//M06-2X/aug-cc-pVTZ calculations and multi-conformer TST, including empirical corrections to reference experimental data, except for limonene-derived CIs where the values are predicted using a structure–activity relationship. The rate coefficients for  $\text{CH}_2\text{OO}$ ,  $\text{CH}_3\text{CHOO}$  and  $(\text{CH}_3)_2\text{COO}$  are within a factor of 4 of evaluated literature data (Vereecken et al., 2017).

Carbonyl oxide	$k(298\text{K}) \text{H}_2\text{O}$	$k(298\text{K}) (\text{H}_2\text{O})_2$
$\text{CH}_2\text{OO}$	$8.7 \times 10^{-16}$	$1.4 \times 10^{-12}$
<i>syn</i> - $\text{CH}_3\text{CHOO}$	$6.7 \times 10^{-19}$	$2.1 \times 10^{-15}$
<i>anti</i> - $\text{CH}_3\text{CHOO}$	$2.3 \times 10^{-14}$	$2.7 \times 10^{-11}$
$(\text{CH}_3)_2\text{COO}$	$7.5 \times 10^{-18}$	$1.8 \times 10^{-14}$
$\alpha$ -pinene		
CI-1a	$1.3 \times 10^{-18}$	$2.9 \times 10^{-15}$
CI-1b	$1.5 \times 10^{-14}$	$1.7 \times 10^{-11}$
CI-2a	$1.0 \times 10^{-18}$	$2.5 \times 10^{-15}$
CI-2b	$2.4 \times 10^{-19}$	$7.0 \times 10^{-16}$
$\beta$ -pinene		
CI-3	$1.7 \times 10^{-18}$	$4.3 \times 10^{-15}$
CI-4	$4.2 \times 10^{-16}$	$6.4 \times 10^{-13}$
Limonene		
CI-5a	$1.5 \times 10^{-18}$	$4.3 \times 10^{-15}$
CI-5b	$1.5 \times 10^{-14}$	$1.7 \times 10^{-11}$
CI-6a	$9.1 \times 10^{-18}$	$2.1 \times 10^{-14}$
CI-6b	$1.5 \times 10^{-17}$	$3.2 \times 10^{-14}$
CI-7a	$9.7 \times 10^{-18}$	$1.9 \times 10^{-14}$
CI-7b	$4.3 \times 10^{-18}$	$1.1 \times 10^{-14}$

$\alpha$ -pinene ozonolysis experiments may consist of a mixture of C-1a, CI-2a and CI-2b.

## 6.2 $\beta$ -pinene

The theoretical analysis for nopinone oxides shows one isomer, SCI-4, that has a fast rate of reaction with water, but a slow unimolecular isomerisation, while the other isomer, SCI-3, shows a fast unimolecular decomposition. These can thus be unequivocally equated to the experimentally obtained SCI-A and SCI-B, respectively, inasmuch as the yield of  $\text{CH}_2\text{OO}$  is minor. The predicted rate coefficients are within the expected uncertainty intervals of the theoretical data, a factor of 5 for the unimolecular rates and an order of magnitude for the reaction with  $\text{H}_2\text{O}$ .

The experimental rate measurements are defined relative to the reaction rate with  $\text{SO}_2$ ; the value adopted for the  $k(\text{SCI} + \text{SO}_2)$  reaction therefore influences the derived rate coefficient values. Ahrens et al. (2014) directly measured the  $\text{SO}_2$  rate coefficient of the longest-lived SCI (SCI-4) to

be  $\sim 4 \times 10^{-11} \text{ cm}^3 \text{ s}^{-1}$ , but for SCI-3 we assume a similar rate coefficient as *syn*- $\text{CH}_3\text{CHOO} + \text{SO}_2$  determined by Sheps et al. (2014) of  $2.9 \times 10^{-11} \text{ cm}^3 \text{ s}^{-1}$ . Nopinone oxides are bicyclic compounds, with a bulky dimethyl-substituted 4-membered ring adjacent to the carbonyl oxide moiety. To examine the potential impact of steric hindrance on the  $\text{SCI} + \text{SO}_2$  reaction, we characterised all sulfur-substituted secondary ozonides (S-SOZ) formed in this reaction (Kuwata et al., 2015; Vereecken et al., 2012). We find that the tricyclic S-SOZ shows very little interaction between the sulfur-bearing ring and the  $\beta$ -pinene substituents, and little change in the ring strain. The energies of the S-SOZ adducts relative to the  $\text{SCI} + \text{SO}_2$  reactants thus remain very similar to that of  $\text{CH}_2\text{OO}$ ,  $\text{CH}_3\text{CHOO}$  or  $(\text{CH}_3)_2\text{COO}$ , confirming the quality of our selection of reference rate coefficients.

## 6.3 Limonene

Of the six non- $\text{CH}_2\text{OO}$  CIs formed in limonene ozonolysis, CI-5b was predicted to have a fast reaction rate with  $\text{H}_2\text{O}$ ; its oxide substitution patterns is similar to pinonaldehyde oxide CI-1b. The SAR-predicted rate coefficient of  $\text{CI-5b} + \text{H}_2\text{O}$  is within a factor of 2 of the experimentally derived  $k_3$  value for SCI-A, such that we can equate SCI-A to CI-5b with confidence. The SCI-B set of Criegee intermediates then contains the summed population of the remaining five CIs, all of which react slowly with  $\text{H}_2\text{O}$ . The SAR-predicted unimolecular decay rate coefficients range from 15 to  $700 \text{ s}^{-1}$ , all within a factor of 9 of the experimentally obtained  $k_d = 130 \text{ s}^{-1}$ ; it should be noted that for limonene-derived CIs, no explicit theoretical calculations are available, and the SAR-predictions carry a somewhat larger uncertainty. We have performed an exhaustive characterisation of the conformers of CI-5b. The most stable conformers show an internal complex formation between the oxide moiety and the carbonyl group, similar to those characterised for the bimolecular reaction of CIs with carbonyl compounds (Jalan et al., 2013; Wei et al., 2015). The theoretical study by Jiang et al. (2013) on limonene ozonolysis appears to have omitted internal rotation and cannot be compared directly. It seems likely that the limonene-derived CIs can thus easily undergo internal SOZ formation, which is thought (Vereecken and Francisco, 2012) to be entropically unfavourable, but has a low barrier to reaction. For  $\alpha$ -pinene, a similar internal complex formation and SOZ ring closure is not as favourable due to the geometric limitations enforced by the 4-membered ring.

A large number of transition state conformers for  $\text{CI-5b} + \text{H}_2\text{O}$  were characterised, though no exhaustive search was completed. The energetically most favourable structures show interaction between the carbonyl group and the  $\text{H}_2\text{O}$  co-reactant as it adds onto the carbonyl oxide moiety. Similar stabilising interactions between the carbonyl moiety and the carbonyl oxide moiety were reported recently in cyclohexene-derived CIs (Berndt et al., 2017). This in-

**Table 5.** Kinetic parameters used in the global modelling study.

SCI	$\varphi_{SCI}$	$10^{15}k_3$ (cm <sup>3</sup> s <sup>-1</sup> )	$10^{11}k_2^a$ (cm <sup>3</sup> s <sup>-1</sup> )	$k_d$ (s <sup>-1</sup> )
<i>α</i> -pinene				
SCI-A	0.08	310	22	–
SCI-B	0.11	–	2.9	240
<i>β</i> -pinene				
SCI-A	0.25	4	4	–
SCI-B	0.35	–	2.9	170
Limonene				
SCI-A	0.05	7.7	22	–
SCI-B	0.18	–	2.9	130
Myrcene				
SCI-B	0.30	–	13 <sup>b</sup>	400 <sup>c</sup>
Ocimene				
SCI-B	0.30	–	13 <sup>b</sup>	400 <sup>c</sup>
Sabinene <sup>d</sup>				
SCI-A	0.25	4	4	–
SCI-B	0.35	–	2.9	170
3-carene <sup>e</sup>				
SCI-A	0.08	310	22	–
SCI-B	0.11	–	2.9	240

<sup>a</sup> $k_2$ (SCI-A + SO<sub>2</sub>) from (SO<sub>2</sub>+*anti*-CH<sub>3</sub>CHOO) – Sheps et al. (2014);  $k_2$ (SCI-B + SO<sub>2</sub>) from (SO<sub>2</sub>+*syn*-CH<sub>3</sub>CHOO) – Sheps et al. (2014) unless otherwise stated. <sup>b</sup> $k_2$ (SCI-B + SO<sub>2</sub>) from (SO<sub>2</sub>+*anti*-(CH<sub>3</sub>)<sub>2</sub>COO) – Huang et al. (2015). <sup>c</sup> Temperature-dependent  $k_d$ (SCI-B) taken from IUPAC (2017). <sup>d</sup> Kinetics based on *β*-pinene. <sup>e</sup> Kinetics based on *α*-pinene.

teraction thus lowers the barrier to a reaction, though it is currently unclear whether it enhances the reaction rate, e.g. compared to the *α*-pinene-derived CI-1b, as these hydrogen-bonded structures are entropically not very favourable. The intra-molecular interactions with heterosubstituents could be investigated in future work.

## 7 Global modelling study

### 7.1 SCI chemistry

A global atmospheric modelling study was performed using the GEOS-Chem chemical transport model (as described in Sect. 4) to examine the global monoterpene-derived SCI budget and the contribution of these SCIs to gas-phase SO<sub>2</sub> oxidation. The existing chemistry scheme in the model is supplemented with monoterpene SCI chemistry based on the experimental results described in Sect. 5 and in Table 5. It should be noted here that this modelling study focuses on the chemical impacts of monoterpene SCIs formed from ozonolysis reactions only. No chemistry for other SCIs derived from

isoprene and/or other (smaller) alkenes are incorporated in the adapted model chemical scheme.

The monoterpene emissions in GEOS-Chem are taken from MEGAN v2.1 (Guenther et al., 2012). The scheme emits seven monoterpenes: *α*-pinene, *β*-pinene, limonene, myrcene, ocimene, 3-carene and sabinene. The monoterpenes are oxidised within the model by OH, NO<sub>3</sub> and O<sub>3</sub> at rates shown in Table S1. Reaction with O<sub>3</sub> leads to the production of monoterpene-specific SCI. Reactions with OH and NO<sub>3</sub> do not lead to the formation of any products, with the reactions only acting as a sink for the monoterpene and the respective oxidant. The SCI yields from the ozonolysis of *α*-pinene, *β*-pinene and limonene are derived from the experimental work presented here. SCIs from each monoterpene are split into SCI-A and SCI-B as defined in previous sections. For the other four monoterpenes emitted, the SCI yields and kinetics are derived based on the similarity of the structure to one of the species studied here or previously in the literature. The main SCIs produced in the ozonolysis of myrcene and ocimene are expected to be acetone oxide ((CH<sub>3</sub>)<sub>2</sub>COO) or 4-vinyl-5-hexenal oxide (CH<sub>2</sub>CHC(CH<sub>2</sub>)CH<sub>2</sub>CH<sub>2</sub>CHOO), since ozone has been sug-

**Table 6.** Monoterpene contribution to [SCI] and SO<sub>2</sub> oxidation in the surface layer of the model simulation.

Monoterpene	Annual emissions* (Tg C)	% contribution to [SCI-A]	% contribution to [SCI-B]	% contribution to SO <sub>2</sub> oxidation
$\alpha$ -pinene	35.4	0.5	15	5.8
$\beta$ -pinene	16.9	74	43	54
Limonene	9.2	3.5	13	6.0
Myrcene	3.1	0.0	2.7	9.0
Trans- $\beta$ -ocimene	14.1	0.0	11	20
Sabinene	7.9	22	13	3.8
3-carene	6.4	0.0	2.5	1.3

\* From MEGAN v2.1 (Guenther et al., 2012).

gested to react predominantly at the internal double bond ( $\sim 97\%$  for myrcene,  $\sim 90\%$  for ocimene Baker et al., 2004). The SCI yield is taken to be 0.30, similar to that of (CH<sub>3</sub>)<sub>2</sub>COO from 2,3-dimethyl-but-2-ene ozonolysis (Newland et al., 2015a). However, this may be an underestimation since it has been predicted that stabilisation of small CIs increase with the size of the carbonyl co-product, as this co-product can take more of the nascent energy of the primary ozonide on decomposition due to a greater number of degrees of freedom available (Nguyen et al., 2009a; Newland et al., 2015b). Sabinene is a bicyclic monoterpene with an external double bond and hence is treated like  $\beta$ -pinene. This assumption is backed up by recent theoretical work (Wang and Wang, 2017), who predict similar behaviour from sabinene-derived SCIs to the predicted behaviour from  $\beta$ -pinene SCIs by Nguyen et al. (2009a). They predict a SCI yield between 24 and 64%. 3-carene is a bicyclic monoterpene with an internal double bond and is treated like  $\alpha$ -pinene.

## 7.2 Modelling results

Figure 7 shows the annually averaged total SCI burden from monoterpene ozonolysis in the surface layer in the GEOS-Chem simulation. A number of interesting features are apparent from this figure and the associated information is given in Table 6:

- The highest annually averaged monoterpene SCI concentrations are found above tropical forests.
- Peak annually averaged monoterpene SCI concentrations are  $\sim 1.4 \times 10^4 \text{ cm}^{-3}$ .
- $>97\%$  of the total monoterpene SCI burden is SCI-B.

Annual global monoterpene emissions are dominated by the tropics (Fig. S1 in the Supplement), accounting for  $>90\%$  during the Northern Hemisphere winter months (November–April) and 70% even during the peak emissions from the northern boreal region during June and July (Sindelarova et al., 2014). Despite annually averaged surface ozone mixing ratios being roughly a factor of 2 higher in the northern middle to high latitudes, monoterpene SCI production

is still dominated by the tropics. Annually averaged surface monoterpene SCI concentrations across the northern boreal regions are  $<2 \times 10^3 \text{ cm}^{-3}$ ; during the summer months (JJA) this value rises to  $2\text{--}5 \times 10^3 \text{ cm}^{-3}$ .

More than 97% of the total monoterpene-derived SCIs are SCI-B (Table 6). This is because typical water vapour concentrations in the tropics are  $>5.0 \times 10^{17} \text{ cm}^{-3}$ . This gives SCI-A removal rates (i.e.  $k_3[\text{H}_2\text{O}]$ ) of  $2 \times 10^3\text{--}1.5 \times 10^5 \text{ s}^{-1}$ , whereas removal rates of SCI-B to unimolecular reactions have been determined here to be 1–3 orders of magnitude slower, of the order of  $100\text{--}250 \text{ s}^{-1}$ . Since the loss of SCI-B is independent of temperature in the model, the highest SCI-B concentrations would be expected to be located in the regions of highest SCI-B production. Recent experimental studies (Smith et al., 2016) have demonstrated a strong temperature dependence for the unimolecular decomposition rate of (CH<sub>3</sub>)<sub>2</sub>COO between 283 and 323 K ( $269\text{--}916 \text{ s}^{-1}$ ). Therefore, it may be that in reality there would be some geographical variation in the rate of unimolecular loss.

The monoterpene SCI-A + H<sub>2</sub>O reactions are expected to lead to high yields of both large (e.g. Ma et al., 2008; Ma and Marston, 2008) and small (measured in high yield in the experiments presented here) organic acids.

Figure 8 shows the seasonal removal of SO<sub>2</sub> by reaction with monoterpene-derived SCI, as a percentage of total gas-phase SO<sub>2</sub> oxidation in the surface layer. Monoterpene SCIs are most important (relative to OH) for SO<sub>2</sub> oxidation over tropical forests, where they account for up to 60% of the local gas-phase SO<sub>2</sub> removal during DJF and MAM in some regions. The reasons for this are two-fold: firstly, the highest modelled monoterpene SCI concentrations are found in these regions (Fig. 7); additionally, OH concentrations in the model are low over these areas (Fig. S2). Historically there have been discrepancies between modelled and observed OH concentrations over tropical forests, with models appearing to underpredict [OH] by up to a factor of 10 (e.g. Lelieveld et al., 2008). It was proposed that this was due to missing sources of OH recycling during isoprene oxidation. During recent years there have been advances in our understanding of isoprene chemistry. GEOS-Chem v-

09, used here, includes an isoprene OH recycling scheme largely based on Paulot et al. (2009a, b), with updates from Peeters et al. (2009), Peeters and Müller (2010) and Crouse et al. (2011, 2012), and evaluated in Mao et al. (2013). However, more recent experimental and theoretical work is not yet included.

Annually, monoterpene SCI oxidation accounts for 1.2 % of the gas-phase SO<sub>2</sub> oxidation in the terrestrial tropics. This accounts for the removal of 2.9 Gg of SO<sub>2</sub>. Across the northern boreal forests, monoterpene SCIs contribute 0.7 % to gas-phase SO<sub>2</sub> removal annually, removing 0.8 Gg of SO<sub>2</sub>. Globally, throughout the whole of the atmosphere, monoterpene SCIs account for only 0.5 % of gas-phase SO<sub>2</sub> removal, removing 8.1 Gg of SO<sub>2</sub> annually.

It is noted that MEGAN does not contain oceanic monoterpene emissions, which may increase the global importance of SCIs for gas-phase SO<sub>2</sub> removal. Luo and Yu (2010) determined annual global oceanic  $\alpha$ -pinene emissions to be 29.5 TgC using a top-down approach, with only 0.013 (Luo and Yu, 2010) – 0.26 (Hackenberg et al., 2017) TgC estimated using a range of bottom-up approaches; clearly there are large uncertainties in oceanic monoterpene emissions. At the upper end of this range they could potentially provide a similar contribution to SCI production and subsequent SO<sub>2</sub> oxidation as monoterpenes emitted from the terrestrial biosphere. SCI production could more generally be further amplified by sources such as marine-derived alkyl iodine photolysis.

Blitz et al. (2017) recently calculated a revised SO<sub>2</sub> + OH reaction rate ( $k_1(1 \text{ bar N}_2)(298 \text{ K}) = 5.8 \times 10^{-13} \text{ cm}^3 \text{ s}^{-1}$ ), based on experimental work and a master equation analysis, which is  $\sim 40\%$  lower than the rate given in the most recent JPL data evaluation (Burkholder et al., 2015) ( $k_1(1 \text{ bar N}_2)(298 \text{ K}) = 9.5 \times 10^{-13} \text{ cm}^3 \text{ s}^{-1}$ ), which is used in the GEOS-Chem model simulation. Figure S3 shows the increased influence of monoterpene-derived SCIs on gas-phase SO<sub>2</sub> oxidation if the alternative SO<sub>2</sub> + OH rate is used. This increased the impact of monoterpene SCIs to up to 67 % of gas-phase SO<sub>2</sub> removal in regions of the tropical forests during DJF and MAM, with the contribution of monoterpene SCIs to global gas-phase SO<sub>2</sub> oxidation increasing to 0.7 %.

While certain monoterpenes appear to be more important than others with regard to the production of SCIs which will oxidise SO<sub>2</sub>, these results are sensitive to the kinetics used and the assumptions made for the monoterpenes not studied experimentally here. Hence we do not attempt to draw any conclusions about the relative importance of each monoterpene from the modelling. Clearly the most important monoterpenes will be those with high yields of SCI-B, particularly if those SCI-B have a structure that hinders unimolecular decomposition (such as certain  $\beta$ -pinene-derived SCI).

## 8 Conclusions

We report results from an integrated experimental (simulation chamber), theoretical (quantum chemical) and modelling (global chemistry-transport simulation) study of the impacts of monoterpene ozonolysis reactions on stabilised Criegee intermediate (SCI) formation and SO<sub>2</sub> oxidation. The ozonolysis of the monoterpenes  $\alpha$ -pinene,  $\beta$ -pinene and limonene have been shown to produce a structurally diverse range of chemically distinct SCIs, with some showing limited sensitivity to reaction with water vapour under near-atmospheric humidity levels. A multi-component system is required to explain the experimentally observed SO<sub>2</sub> removal kinetics. A two-body model system based on the assumption of a fraction of the SCIs produced being reactive towards water (SCI-A; potentially contributing to the significant formation of a range of organic acids in the atmosphere) and a fraction being relatively unreactive towards water (SCI-B), analogous to the structural dependencies observed for the simpler CH<sub>3</sub>CHOO SCI system, has been shown to describe the observed kinetic data reasonably well for all the monoterpene systems investigated and may form a computationally affordable and conceptually accessible basis for the description of this chemistry within atmospheric models. Moreover such an approach is required to accurately predict SCI concentrations, which will be underestimated if a simple average of the properties of the two different SCI classes is used. The atmospheric fate of SCI-B produced from the monoterpenes studied here will be controlled by their removal by unimolecular decomposition. In this work, we have experimentally determined the monoterpene SCI-B decomposition rate to be between 100 and 250 s<sup>-1</sup>. This has significant implications for the role of monoterpene-derived SCIs as oxidants in the atmosphere. The fate of SCI-A will be reaction with water or the water dimer, likely leading to the production of a range of organic acids.

A theory-based analysis of the kinetics of the SCIs formed from  $\alpha$ -pinene,  $\beta$ -pinene ozonolysis has also been performed, which complements the experimental work. The identification of the likely SCI-A and SCI-B populations and the derived kinetics agree with experimental observations within the respective uncertainties.

A modelling study using the GEOS-Chem global 3-D chemical transport model supplemented with the chemical kinetics elucidated in this work suggests that the global monoterpene-derived SCI burden will be dominated (>97 %) by SCI-B. The highest annually averaged SCI concentrations are found in the tropics, with seasonally averaged monoterpene SCI concentrations up to  $1.4 \times 10^4 \text{ cm}^{-3}$  owing to large monoterpene emissions. Across the boreal forest, average SCI concentrations reach between 3 and  $5 \times 10^3 \text{ cm}^{-3}$  during the Northern Hemisphere summer. Oxidation of SO<sub>2</sub> by monoterpene SCIs is shown to also be most important in the tropics. While oxidation by SCIs contributes <1% to gas-phase SO<sub>2</sub> oxidation globally, over tropical forests this can

rise to up to 60 % at certain times of the year. Monoterpene SCI-driven SO<sub>2</sub> oxidation will increase the production of sulfate aerosol – affecting atmospheric radiation transfer and hence climate – and reduce the atmospheric lifetime and hence the transport of SO<sub>2</sub>. These effects will be substantial in areas where monoterpene emissions are significant, in particular over the Amazon, central Africa and SE Asian rainforests.

*Data availability.* Experimental data and GEOS-Chem model output are available at <https://doi.org/10.15124/4e9cd832-9cce-41c8-8335-c88cf32fe244> (Newland et al., 2013), and will subsequently also be available in the Eurochamp database ([www.eurochamp.org](http://www.eurochamp.org), last access: 27 April 2018) from the H2020 EUROCHAMP2020 project, GA no. 730997. GEOS-Chem model code is available at <https://doi.org/10.5281/zenodo.1220385> and the model run directory is available at <https://doi.org/10.5281/zenodo.1220387> (GEOS-Chem team v9-02, 2018).

**The Supplement related to this article is available online at <https://doi.org/10.5194/acp-18-6095-2018-supplement>.**

*Competing interests.* The authors declare that they have no conflict of interest.

*Acknowledgements.* The assistance of the EUPHORE staff is gratefully acknowledged. Salim Alam, Marie Camredon and Stephanie La are thanked for helpful discussions. This work was funded by EU FP7 EUROCHAMP 2 Transnational Access activity (E2-2012-05-28-0077) and the UK NERC projects NE/K005448/1, Reactions of Stabilised Criegee Intermediates in the Atmosphere: Implications for Tropospheric Composition & Climate NE/M013448/1, Mechanisms for Atmospheric chemistry: GenerationN, Interpretation and Fidelity – MAGNIFY. Fundación CEAM is partly supported by Generalitat Valenciana, and the project DESESTRES (Prometeo Program – Generalitat Valenciana). EUPHORE instrumentation is partly funded by the Spanish Ministry of Science and Innovation through the INNPLANTA project PCT-440000-2010-003. Luc Vereecken is indebted to the Max Planck Graduate Center and the Johannes Gutenberg-Universität Mainz (MPGC).

Edited by: Robert McLaren

Reviewed by: three anonymous referees

## References

Ahrens, J., Carlsson, P. T. M., Hertl, N., Olzmann, M., Pfeifle, M., Wolf, J. L., and Zeuch, T.: Infrared Detection of Criegee Intermediates Formed during the Ozonolysis of  $\beta$ -pinene and Their Reactivity towards Sulfur Dioxide, *Angew. Chem. Int. Edit.*, 53, 715–719, 2014.

- Alam, M. S., Camredon, M., Rickard, A. R., Carr, T., Wyche, K. P., Hornsby, K. E., Monks, P. S., and Bloss, W. J.: Total radical yields from tropospheric ethene ozonolysis, *Phys. Chem. Chem. Phys.*, 13, 11002–11015, 2011.
- Alam, M. S., Rickard, A. R., Camredon, M., Wyche, K. P., Carr, T., Hornsby, K. E., Monks, P. S., and Bloss, W. J.: Radical Product Yields from the Ozonolysis of Short Chain Alkenes under Atmospheric Boundary Layer Conditions, *J. Phys. Chem. A*, 117, 12468–12483, 2013.
- Anglada, J. M., Gonzalez, J., and Torrent-Sucarrat, M.: Effects of the substituents on the reactivity of carbonyl oxides. A theoretical study on the reaction of substituted carbonyl oxides with water, *Phys. Chem. Chem. Phys.*, 13, 13034–13045, 2011.
- Anglada, M. and Sole, A.: Impact of the water dimer on the atmospheric reactivity of carbonyl oxides, *Phys. Chem. Chem. Phys.*, 18, 17698–17712, 2016.
- Asatryan, R. and Bozzelli, J.W.: Formation of a Criegee intermediate in the low-temperature oxidation of dimethyl sulfoxide, *Phys. Chem. Chem. Phys.*, 10, 1769–1780, 2008.
- Baptista, L., Pfeifer, L., da Silva, E. C., and Arbilla, G.: Kinetics and Thermodynamics of Limonene Ozonolysis, *J. Phys. Chem. A*, 115, 10911–10919, 2011.
- Baker, J., Arey, J., and Atkinson, R.: Kinetics of the gas-phase reactions of OH radicals, NO<sub>3</sub> radicals and O<sub>3</sub> with three C7-carbonyls formed from the atmospheric reactions of myrcene, ocimene and terpinolene, *J. Atmos. Chem.*, 48, 241–260, 2004.
- Beck, M., Winterhalter, R., Herrmann, F., and Moortgat, G. K.: The gas-phase ozonolysis of  $\alpha$ -humulene, *Phys. Chem. Chem. Phys.*, 13, 10970–11001, 2011.
- Becker, K. H.: EUPHORE: Final Report to the European Commission, Contract EV5V-CT92-0059, Bergische Universität Wuppertal, Germany, 1996.
- Berndt, T., Voigtländer, J., Stratmann, F., Junninen, H., Mauldin III, R. L., Sipilä, M., Kulmala, M., and Herrmann, H.: Competing atmospheric reactions of CH<sub>2</sub>OO with SO<sub>2</sub> and water vapour, *Phys. Chem. Chem. Phys.*, 16, 19130–19136, 2014.
- Berndt, T., Kaethner, R., Voigtländer, J., Stratmann, F., Pfeifle, M., Reichle, P., Sipilä, M., Kulmala, M., and Olzmann, M.: Kinetics of the unimolecular reaction of CH<sub>2</sub>OO and the bimolecular reactions with the water monomer, acetaldehyde and acetone at atmospheric conditions, *Phys. Chem. Chem. Phys.*, 17, 19862–19873, 2015.
- Berndt, T., Herrmann, H., and Kurtén, T.: Direct probing of Criegee intermediates from gas-phase ozonolysis using chemical ionization mass spectrometry, *J. Am. Chem. Soc.*, 139, 13387–13392, <https://doi.org/10.1021/jacs.7b05849>, 2017.
- Berresheim, H., Adam, M., Monahan, C., O'Dowd, C., Plane, J. M. C., Bohn, B., and Rohrer, F.: Missing SO<sub>2</sub> oxidant in the coastal atmosphere? – observations from high-resolution measurements of OH and atmospheric sulfur compounds, *Atmos. Chem. Phys.*, 14, 12209–12223, <https://doi.org/10.5194/acp-14-12209-2014>, 2014.
- Bey, I., Jacob, D. J., Yantosca, R. M., Logan, J. A., Field, B. D., Fiore, A. M., Li, Q., Liu, H. Y., Mickley, L. J., and Schultz, M. G.: Global modelling of tropospheric chemistry with assimilated meteorology: Model description and evaluation, *J. Geophys. Res.*, 106, 23073–23095, 2001.
- Blitz, M. A., Salter, R. J., Heard, D. E., and Seakins, P. J.: An Experimental and Master Equation Study of the Kinetics of

- OH / OD + SO<sub>2</sub>: The Limiting High-Pressure Rate Coefficients, *J. Phys. Chem. A*, 121, 3184–3191, 2017.
- Burkholder, J. B., Sander, S. P., Abbatt, J., Barker, J. R., Huie, R. E., Kolb, C. E., Kurylo, M. J., Orkin, V. L., Wilmouth, D. M., and Wine, P. H.: Chemical Kinetics and Photochemical Data for Use in Atmospheric Studies, Evaluation No. 18, JPL Publication 15–10, Jet Propulsion Laboratory, Pasadena, available at: <http://jpldataeval.jpl.nasa.gov> (last access: 27 April 2018), 2015.
- Caravan, R. L., Khan, A. H. M., Rotavera, B., Papajak, E., Antonov, I. O., Chen, M.-W., Au, K., Chao, W., Osborn, D. L., Lin, J. J.-M., Percival, C. J., Shallcross, D. E., and Taatjes, C. E.: Products of Criegee intermediate reactions with NO<sub>2</sub>: experimental measurements and tropospheric implications, *Faraday Discuss.*, 200, 313–330, 2017.
- Chang, Y.-P., Chang, H.-H., and Lin, J. J.-M.: Kinetics of the simplest Criegee intermediate reaction with ozone studied using a mid-infrared quantum cascade laser spectrometer, *Phys. Chem. Chem. Phys.*, 20, 97–102, <https://doi.org/10.1039/c7cp06653h>, 2018.
- Chao, W., Hsieh, J.-T., Chang, C.-H., and Lin, J. J.-M.: Direct kinetic measurement of the reaction of the simplest Criegee intermediate with water vapour, *Science*, 347, 751–754, <https://doi.org/10.1126/science.1261549>, 2015.
- Chen, L., Wang, W., Wang, W., Liu, Y., Liu, F., Liu, N., and Wang, B.: Water-catalyzed decomposition of the simplest Criegee intermediate CH<sub>2</sub>OO, *Theor. Chem. Acc.*, 135, 131, <https://doi.org/10.1007/s00214-016-1894-9>, 2016.
- Chhantyal-Pun, R., Davey, A., Shallcross, D. E., Percival, C. J., and Orr-Ewing, A. J.: A kinetic study of the CH<sub>2</sub>OO Criegee intermediate self-reaction, reaction with SO<sub>2</sub> and unimolecular reaction using cavity ring-down spectroscopy, *Phys. Chem. Chem. Phys.*, 17, 3617–3626, 2015.
- Chhantyal-Pun, R., Welz, O., Savee, J. D., Eskola, A. J., Lee, E. P. F., Blacker, L., Hill, H. R., Ashcroft, M., Khan, M. A. H. H., Lloyd-Jones, G. C., Evans, L. A., Rotavera, B., Huang, H., Osborn, D. L., Mok, D. K. W., Dyke, J. M., Shallcross, D. E., Percival, C. J., Orr-Ewing, A. J., and Taatjes, C. A.: Direct Measurements of Unimolecular and Bimolecular Reaction Kinetics of the Criegee Intermediate (CH<sub>3</sub>)<sub>2</sub>COO, *J. Phys. Chem. A*, 121, 4–15, 2017.
- Chuong, B., Zhang, J., and Donahue, N. M.: Cycloalkene Ozonolysis: Collisionally Mediated Mechanistic Branching, *J. Am. Chem. Soc.*, 126, 12363–12373, 2004.
- Cox, R. A. and Penkett, S. A.: Oxidation of atmospheric SO<sub>2</sub> by products of the ozone-olefin reaction, *Nature*, 230, 321–322, 1971.
- Crouse, J. D., Paulot, F., Kjaergaard, H. G., and Wennberg, P. O.: Peroxy radical isomerization in the oxidation of isoprene, *Phys. Chem. Chem. Phys.*, 13, 13607–13613, 2011.
- Crouse, J. D., Knap, H. C., Ørnsø, K. B., Jørgensen, S., Paulot, F., Kjaergaard, H. G., and Wennberg, P. O.: Atmospheric fate of methacrolein. 1. Peroxy radical isomerization following addition of OH and O<sub>2</sub>, *J. Phys. Chem. A*, 116, 5756–5762, 2012.
- Decker, Z. C. J., Au, K., Vereecken, L., and Sheps, L.: Direct experimental probing and theoretical analysis of the reaction between the simplest Criegee intermediate and CH<sub>2</sub>OO and isoprene, *Phys. Chem. Chem. Phys.*, 19, 8541–8551, 2017.
- Donahue, N. M., Drozd, G. T., Epstein, S. A., Presto, A. A., and Kroll, J. H.: Adventures in ozoneland: down the rabbit-hole, *Phys. Chem. Chem. Phys.*, 13, 10848–10857, 2011.
- Drozd, G. T. and Donahue, N. M.: Pressure Dependence of Stabilized Criegee Intermediate Formation from a Sequence of Alkenes, *J. Phys. Chem. A*, 115, 4381–4387, 2011.
- Eckart, C.: The penetration of a potential barrier by electrons, *Phys. Rev.*, 35, 1303–1309, 1930.
- Ehn, M., Thornton, J. A., Kleist, E., Sipilä, M., Junninen, H., Pulli-nen, I., Springer, M., Rubach, F., Tillmann, R., Lee, B., Lopez-Hilfiker, F., Andres, S., Acir, I.-H., Rissanen, M., Jokinen, T., Schobesberger, S., Kangasluoma, J., Kontkanen, J., Nieminen, T., Kurtein, T., Nielsen, L. B., Jørgensen, S., Kjaergaard, H. G., Canagaratna, M., Maso, M. D., Berndt, T., Petäjä, T., Wahner, A., Kerminen, V.-M., Kulmala, M., Worsnop, D. R., Wildt, J., and Mentel, T. F.: A large source of low-volatility secondary organic aerosol, *Nature*, 506, 476–479, <https://doi.org/10.1038/nature13032>, 2014.
- Fang, Y., Liu, F., Barber, V. P., Klippenstein, S. J., McCoy, A. B., and Lester, M. I.: Communication: Real time observation of unimolecular decay of Criegee intermediates to OH radical products, *J. Chem. Phys.*, 144, 061102, <https://doi.org/10.1063/1.4941768>, 2016a.
- Fang, Y., Liu, F., Klippenstein, S. J., and Lester, M. I.: Direct observation of unimolecular decay of CH<sub>3</sub>CH<sub>2</sub>CHOO Criegee intermediates to OH radical products, *J. Chem. Phys.*, 145, 044312, <https://doi.org/10.1063/1.4958992>, 2016b.
- Fenske, J. D., Hasson, A. S., Ho, A. W., and Paulson, S. E.: Measurement of absolute unimolecular and bimolecular rate constants for CH<sub>3</sub>CHOO generated by the trans-2-butene reaction with ozone in the gas phase, *J. Phys. Chem. A*, 104, 9921–9932, 2000.
- Foreman, E. S., Kapnas, K. M., and Murray, C.: Reactions between Criegee Intermediates and the Inorganic Acids HCl and HNO<sub>3</sub>: Kinetics and Atmospheric Implications, *Angew. Chem. Int. Edit.*, 55, 1–5, 2016.
- Frisch, M. J., Trucks, G. W., Schlegel, H. B., Scuseria, G. E., Robb, M. A., Cheeseman, J. R., Scalmani, G., Barone, V., Mennucci, B., Petersson, G. A., Nakatsuji, H., Caricato, M., Li, X., Hratchian, H. P., Izmaylov, A. F., Bloino, J., Zheng, G., Sonnenberg, J. L., Hada, M., Ehara, M., Toyota, K., Fukuda, R., Hasegawa, J., Ishida, M., Nakajima, T., Honda, Y., Kitao, O., Nakai, H., Vreven, T., Montgomery Jr., J. A., Peralta, J. E., Ogliaro, F., Bearpark, M., Heyd, J. J., Brothers, E., Kudin, K. N., Staroverov, V. N., Keith, T., Kobayashi, R., Normand, J., Normand, J., Raghavachari, K., Rendell, A., Burant, J. C., Iyengar, S. S., Tomasi, J., Cossi, M., Rega, N., Millam, J. M., Klene, M., Knox, J. E., Cross, J. B., Bakken, V., Adamo, C., Jaramillo, J., Gomperts, R., Stratmann, R. E., Yazyev, O., Austin, A. J., Cammi, R., Pomelli, C., Ochterski, J. W., Martin, R. L., Morokuma, K., Zakrzewski, V. G., Voth, G. A., Salvador, P., Dannenberg, J. J., Dapprich, S., Daniels, A. D., Farkas, O., Foresman, J. B., Ortiz, J. V., Cioslowski, J., Fox, D. J., and Pople, J. A.: Gaussian 09, Revision B.01, Gaussian Inc., Wallington CT, 2010.
- GEOS-Chem team v9-02: Newland et al. (2018) ACP, <https://doi.org/10.5281/zenodo.1220387>, 2018.

- Gravestock, T. J., Blitz, M. A., Bloss, W. J., and Heard, D. E.: A multidimensional study of the reaction  $\text{CH}_2\text{I}+\text{O}_2$ : Products and atmospheric implications, *ChemPhysChem*, 1, 3928–3941, 2010.
- Guenther, A., Karl, T., Harley, P., Wiedinmyer, C., Palmer, P. I., and Geron, C.: Estimates of global terrestrial isoprene emissions using MEGAN (Model of Emissions of Gases and Aerosols from Nature), *Atmos. Chem. Phys.*, 6, 3181–3210, <https://doi.org/10.5194/acp-6-3181-2006>, 2006.
- Guenther, A. B., Jiang, X., Heald, C. L., Sakulyanontvittaya, T., Duhl, T., Emmons, L. K., and Wang, X.: The Model of Emissions of Gases and Aerosols from Nature version 2.1 (MEGAN2.1): an extended and updated framework for modeling biogenic emissions, *Geosci. Model Dev.*, 5, 1471–1492, <https://doi.org/10.5194/gmd-5-1471-2012>, 2012.
- Gutbrod, R., Schindler, R. N., Kraka, E., and Cremer, D.: Formation of OH radicals in the gas phase ozonolysis of alkenes: the unexpected role of carbonyl oxides, *Chem. Phys. Lett.*, 252, 221–229, 1996.
- Hackenberg S. C., Andrews, S. J., Airs, R. L., Arnold, S. R., Bouman, H. A., Cummings, D., Lewis, A. C., Minaeian, J. K., Reifel, K. M., Small, A., Tarran, G. A., Tilstone, G. H., and Carpenter, L. J.: Basin-Scale Observations of Monoterpenes in the Arctic and Atlantic Oceans, *Environ. Sci. Technol.*, 51, 10449–10458, 2017.
- Hasson, A. S., Ho, A. W., Kuwata, K. T., and Paulson, S. E.: Production of stabilized Criegee intermediates and peroxides in the gas phase ozonolysis of alkenes 2. Asymmetric and biogenic alkenes, *J. Geophys. Res.*, 106, 34143–34153, 2001.
- Hatakeyama, S., Kobayashi, H., and Akimoto, H.: Gas-Phase Oxidation of  $\text{SO}_2$  in the Ozone-Olefin Reactions, *J. Phys. Chem.*, 88, 4736–4739, 1984.
- Huang, H.-L., Chao, W., and Lin, J. J.-M.: Kinetics of a Criegee intermediate that would survive at high humidity and may oxidize atmospheric  $\text{SO}_2$ , *P. Natl. Acad. Sci. USA*, 112, 10857–10862, 2015.
- IUPAC: Task Group on Atmospheric Chemical Kinetic Data Evaluation – Data Sheet Ox\_VOC20, available at: <http://iupac.pole-ether.fr> (last access: 27 April 2018), 2013.
- IUPAC: Task Group on Atmospheric Chemical Kinetic Data Evaluation – Data Sheet CGI\_14\_((CH<sub>3</sub>)<sub>2</sub>COO + M), available at: <http://iupac.pole-ether.fr> (last access: 27 April 2018), 2017.
- Jalan, A., Allen, J. W., and Green, W. H.: Chemically activated formation of organic acids in reactions of the Criegee intermediate with aldehydes and ketones, *Phys. Chem. Chem. Phys.*, 15, 16841–16852, 2013.
- Jenkin, M. E., Saunders, S. M., and Pilling, M. J.: The tropospheric degradation of volatile organic compounds: a protocol for mechanism development, *Atmos. Environ.*, 31, 81–104, 1997.
- Jenkin, M. E., Young, J. C., and Rickard, A. R.: The MCM v3.3.1 degradation scheme for isoprene, *Atmos. Chem. Phys.*, 15, 11433–11459, <https://doi.org/10.5194/acp-15-11433-2015>, 2015.
- Jiang, L., Lan, R., Xu, Y.-S., Zhang, W.-J., and Yang, W.: Reaction of stabilized criegee intermediates from ozonolysis of limonene with water: Ab initio and DFT study, *Int. J. Mol. Sci.*, 14, 5784–5805, 2013.
- Johnson, D. and Marston, G.: The gas-phase ozonolysis of unsaturated volatile organic compounds in the troposphere, *Chem. Soc. Rev.*, 37, 699–716, 2008.
- Johnston, H. S. and Heicklen, J.: Tunneling corrections for unsymmetrical Eckart potential energy barriers, *J. Phys. Chem.*, 66, 532–533, 1962.
- Kidwell, N. M., Li, H., Wang, X., Bowman, J. M., and Lester, M. I.: Unimolecular dissociation dynamics of vibrationally activated  $\text{CH}_3\text{CHOO}$  Criegee intermediates to OH radical products, *Nat. Chem.*, 8, 509–514, 2016.
- Kirkby, J., Duplissy, J., Sengupta, K., Frege, C., Gordon, H., Williamson, C., Heinritzi, M., Simon, M., Yan, C., Almeida, J., Tröstl, J., Nieminen, T., Ortega, I. K., Wagner, R., Adamov, A., Amorim, A., Bernhammer, A. K., Bianchi, F., Breitenlechner, M., Brilke, S., Chen, X. M., Craven, J., Dias, A., Ehrhart, S., Flagan, R. C., Franchin, A., Fuchs, C., Guida, R., Hakala, J., Hoyle, C. R., Jokinen, T., Junninen, H., Kangasluoma, J., Kim, J., Krapf, M., Kürten, A., Laaksonen, A., Lehtipalo, K., Makhmutov, V., Mathot, S., Molteni, U., Onnela, A., Peräkylä, O., Piel, F., Petäjä, T., Praplan, A. P., Pringle, K., Rap, A., Richards, N. A. D., Riipinen, I., Rissanen, M. P., Rondo, L., Sarnela, N., Schobesberger, S., Scott, C. E., Seinfeld, J. H., Sipilä, M., Steiner, G., Stozhkov, Y., Stratmann, F., Tome, A., Virtanen, A., Vogel, A. L., Wagner, A. C., Wagner, P. E., Weingartner, E., Wimmer, D., Winkler, P. M., Ye, P. L., Zhang, X., Hansel, A., Dommen, J., Donahue, N. M., Worsnop, D. R., Baltensperger, U., Kulmala, M., Carslaw, K. S., and Curtius, J.: Ion-induced nucleation of pure biogenic particles, *Nature*, 533, 521–526, 2016.
- Kjaergaard, H. G., Kurtén, T., Nielsen, L. B., Jørgensen, S., and Wennberg, P. O.: Criegee Intermediates React with Ozone, *J. Phys. Chem. Lett.*, 4, 2525–2529, 2013.
- Kotzias, D., Fytianos, K., and Geiss, F.: Reactions of monoterpenes with ozone, sulphur dioxide and nitrogen dioxide – Gas phase oxidation of  $\text{SO}_2$  and formation of sulphuric acid, *Atmos. Environ.*, 24, 2127–2132, 1990.
- Kroll, J., Donahue, N. M., Cee, V. J., Demerjian, K. L., and Anderson, J. G.: Gas-phase ozonolysis of alkenes: formation of OH from anti carbonyl oxides, *J. Am. Chem. Soc.*, 124, 8518–8519, 2002.
- Kuwata, K. T., Guinn, E., Hermes, M. R., Fernandez, J., Mathison, J., and Huang, K.: A Computational Re-Examination of the Criegee Intermediate-Sulfur Dioxide Reaction, *J. Phys. Chem. A*, 119, 10316–10335, 2015.
- Kuwata, K. T., Hermes, M. R., Carlson, M. J., and Zogg, C. K.: Computational Studies of the Isomerization and Hydration Reactions of Acetaldehyde Oxide and Methyl Vinyl Carbonyl Oxide, *J. Phys. Chem. A*, 114, 9192–9204, 2010.
- Lelieveld, J., Butler, T. M., Crowley, J. N., Dillon, T. J., Fischer, H., Ganzeveld, L., Harder, H., Lawrence, M. G., Martinez, M., Taraborrelli, D., and Williams, J.: Atmospheric oxidation capacity sustained by a tropical forest, *Nature*, 452, 737–740, 2008.
- Leungsakul, S., Jaoui, M., and Kamens, R. M.: Kinetic Mechanism for Predicting Secondary Organic Aerosol Formation from the Reaction of *d*-limonene with Ozone, *Environ. Sci. Technol.*, 39, 9583–9594, 2005.
- Lewis, T. R., Blitz, M. A., Heard, D. E., and Seakins, P. W.: Direct evidence for a substantive reaction between the Criegee intermediate,  $\text{CH}_2\text{OO}$ , and the water vapour dimer, *Phys. Chem. Chem. Phys.*, 17, 4859–4863, 2015.
- Lin, L.-C., Chang, H., Chang, C., Chao, W., Smith, M. C., Chang, C., Lin, J. J., and Takahashi, K.: Competition between  $\text{H}_2\text{O}$  and

- (H<sub>2</sub>O)<sub>2</sub> reactions with CH<sub>2</sub>OO/CH<sub>3</sub>CHOO, *Phys. Chem. Chem. Phys.*, 18, 4557–4568, 2016a.
- Lin, L.-C., Chao, W., Chang, C.-H., Takahashi, K., and Lin, J. J.-M.: Temperature dependence of the reaction of: Anti-CH<sub>3</sub>CHOO with water vapor, *Phys. Chem. Chem. Phys.*, 18, 28189–28197, 2016b.
- Liu, Y., Liu, F., Liu, S., Dai, D., Dong, W., and Yang, X.: A kinetic study of the CH<sub>2</sub>OO Criegee intermediate reaction with SO<sub>2</sub>, (H<sub>2</sub>O)<sub>2</sub>, CH<sub>2</sub>I<sub>2</sub> and I atoms using OH laser induced fluorescence, *Phys. Chem. Chem. Phys.*, 19, 20786–20794, 2017.
- Long, B., Bao, J. L., and Truhlar, D. G.: Atmospheric Chemistry of Criegee Intermediates. Unimolecular Reactions and Reactions with Water, *J. Am. Chem. Soc.*, 138, 14409–14422, 2016.
- Luo, G. and Yu, F.: A numerical evaluation of global oceanic emissions of  $\alpha$ -pinene and isoprene, *Atmos. Chem. Phys.*, 10, 2007–2015, 2010.
- Ma, Y. and Marston, G.: Multi-functional acid formation from the gas-phase ozonolysis of  $\beta$ -pinene, *Phys. Chem. Chem. Phys.*, 10, 6115–6126, 2008.
- Ma, Y., Russell, A. T., and Marston, G.: Mechanisms for the formation of secondary organic aerosol components from the gas-phase ozonolysis of  $\alpha$ -pinene, *Phys. Chem. Chem. Phys.*, 10, 4294–4312, 2008.
- Malkin, T. L., Goddard, A., Heard, D. E., and Seakins, P. W.: Measurements of OH and HO<sub>2</sub> yields from the gas phase ozonolysis of isoprene, *Atmos. Chem. Phys.*, 10, 1441–1459, <https://doi.org/10.5194/acp-10-1441-2010>, 2010.
- Mao, J., Jacob, D. J., Evans, M. J., Olson, J. R., Ren, X., Brune, W. H., Clair, J. M. St., Crouse, J. D., Spencer, K. M., Beaver, M. R., Wennberg, P. O., Cubison, M. J., Jimenez, J. L., Fried, A., Weibring, P., Walega, J. G., Hall, S. R., Weinheimer, A. J., Cohen, R. C., Chen, G., Crawford, J. H., McNaughton, C., Clarke, A. D., Jaeglé, L., Fisher, J. A., Yantosca, R. M., Le Sager, P., and Carouge, C.: Chemistry of hydrogen oxide radicals (HO<sub>x</sub>) in the Arctic troposphere in spring, *Atmos. Chem. Phys.*, 10, 5823–5838, <https://doi.org/10.5194/acp-10-5823-2010>, 2010.
- Mao, J., Paulot, F., Jacob, D. J., Cohen, R. C., Crouse, J. D., Wennberg, P. O., Keller, C. A., Hudman, R. C., Barkley, M. P., and Horowitz, L. W.: Ozone and organic nitrates over the eastern United States: Sensitivity to isoprene chemistry, *J. Geophys. Res.*, 118, 11256–11268, 2013.
- Martinez, R. I. and Herron, J. T.: Stopped-flow studies of the mechanisms of alkene-ozone reactions in the gas-phase: tetramethylethylene, *J. Phys. Chem.*, 91, 946–953, 1987.
- Mauldin III, R. L., Berndt, T., Sipilä, M., Paasonen, P., Petäjä, T., Kim, S., Kurtén, T., Stratmann, F., Kerminen, V.-M., and Kulmala, M.: A new atmospherically relevant oxidant, *Nature*, 488, 193–196, 2012.
- Newland, M. J., Rickard, A. R., Sherwen, T., Evans, M. J., Vereecken, L., Muñoz, A., Ródenas, M., and Bloss, W. J.: Raw data from Newland et al., 2018, ACP, Monoterpene SCI, <https://doi.org/10.15124/4e9cd832-9cce-41c8-8335-c88cf32fe244>, 2013.
- Newland, M. J., Rickard, A. R., Alam, M. S., Vereecken, L., Muñoz, A., Ródenas, M., and Bloss, W. J.: Kinetics of stabilised Criegee intermediates derived from alkene ozonolysis: reactions with SO<sub>2</sub>, H<sub>2</sub>O and decomposition under boundary layer conditions, *Phys. Chem. Chem. Phys.*, 17, 4076–4088, 2015a.
- Newland, M. J., Rickard, A. R., Vereecken, L., Muñoz, A., Ródenas, M., and Bloss, W. J.: Atmospheric isoprene ozonolysis: impacts of stabilised Criegee intermediate reactions with SO<sub>2</sub>, H<sub>2</sub>O and dimethyl sulfide, *Atmos. Chem. Phys.*, 15, 9521–9536, <https://doi.org/10.5194/acp-15-9521-2015>, 2015b.
- Nguyen, T. L., Peeters, J., and Vereecken, L.: Theoretical study of the gas-phase ozonolysis of  $\beta$ -pinene (C<sub>10</sub>H<sub>16</sub>), *Phys. Chem. Chem. Phys.*, 11, 5643–5656, 2009a.
- Nguyen, T. L., Winterhalter, R., Moortgat, G., Kanawati, B., Peeters, J., and Vereecken, L.: The gas-phase ozonolysis of  $\beta$ -caryophyllene (C<sub>15</sub>H<sub>24</sub>). Part II: A theoretical study, *Phys. Chem. Chem. Phys.*, 11, 4173–4183, 2009b.
- Nguyen, T. L., Lee, H., Matthews, D. A., McCarthy, M. C., and Stanton, J. F.: Stabilization of the Simplest Criegee Intermediate from the Reaction between Ozone and Ethylene: A High Level Quantum Chemical and Kinetic Analysis of Ozonolysis, *J. Phys. Chem. A*, 119, 5524–5533, 2015.
- Niki, H., Maker, P. D., Savage, C. M., Breitenbach, L. P., and Hurley, M. D.: FTIR spectroscopic study of the mechanism for the gas-phase reaction between ozone and tetramethylethylene, *J. Phys. Chem.*, 91, 941–946, 1987.
- Novelli, A., Vereecken, L., Lelieveld, J., and Harder, H.: Direct observation of OH formation from stabilised Criegee intermediates, *Phys. Chem. Chem. Phys.*, 16, 19941–19951, 2014.
- Parrella, J. P., Jacob, D. J., Liang, Q., Zhang, Y., Mickley, L. J., Miller, B., Evans, M. J., Yang, X., Pyle, J. A., Theys, N., and Van Roozendaal, M.: Tropospheric bromine chemistry: implications for present and pre-industrial ozone and mercury, *Atmos. Chem. Phys.*, 12, 6723–6740, <https://doi.org/10.5194/acp-12-6723-2012>, 2012.
- Paulot, F., Crouse, J. D., Kjaergaard, H. G., Kürten, A., Clair, J. M. S., Seinfeld, J. H., and Wennberg, P. O.: Unexpected epoxide formation in the gas-phase photooxidation of isoprene, *Science*, 325, 730–733, 2009a.
- Paulot, F., Crouse, J. D., Kjaergaard, H. G., Kroll, J. H., Seinfeld, J. H., and Wennberg, P. O.: Isoprene photooxidation: new insights into the production of acids and organic nitrates, *Atmos. Chem. Phys.*, 9, 1479–1501, <https://doi.org/10.5194/acp-9-1479-2009>, 2009b.
- Paulson, S. E., Chung, M., Sen, A. D., and Orzechowska, G.: Measurement of OH radical formation from the reaction of ozone with several biogenic alkenes, *Geophys. Res. Lett.*, 24, 3193–3196, 1997.
- Peeters, J. and Müller, J. F.: HO<sub>x</sub> radical regeneration in isoprene oxidation via peroxy radical isomerisations. II: Experimental evidence and global impact, *Phys. Chem. Chem. Phys.*, 12, 14227–14235, 2010.
- Peeters, J., Nguyen, T. L., and Vereecken, L.: HO<sub>x</sub> radical regeneration in the oxidation of isoprene, *Phys. Chem. Chem. Phys.*, 11, 5935–5939, 2009.
- Pöschl, U. and Shiraiwa, M.: Multiphase Chemistry at the Atmosphere-Biosphere Interface Influencing Climate and Public Health in the Anthropocene, *Chem. Rev.*, 115, 4440–4475, 2015.
- Rickard, A. R., Johnson, D., McGill, C. D., and Marston, G.: OH Yields in the Gas-Phase reactions of Ozone with Alkenes, *J. Phys. Chem. A*, 103, 7656–7664, 1999.
- Rossignol, S., Rio, C., Ustache, A., Fable, S., Nicolle, J., Mème, A., D'Anna, B., Nicolas, M., Leoz, E., and Chiappini, L.: The use of a housecleaning product in an indoor environment leading

- to oxygenated polar compounds and SOA formation: Gas and particulate phase chemical characterization, *Atmos. Environ.*, 75, 196–205, 2013.
- Ryzhkov, A. B., and Ariya, P. A.: A theoretical study of the reactions of parent and substituted Criegee intermediates with water and the water dimer, *Phys. Chem. Chem. Phys.*, 6, 5042–5050, 2004.
- Sarwar, G. and Corsi, R.: The effects of ozone/limonene reactions on indoor secondary organic aerosols, *Atmos. Environ.*, 41, 959–973, 2007.
- Saunders, S. M., Jenkin, M. E., Derwent, R. G., and Pilling, M. J.: Protocol for the development of the Master Chemical Mechanism, MCM v3 (Part A): tropospheric degradation of non-aromatic volatile organic compounds, *Atmos. Chem. Phys.*, 3, 161–180, <https://doi.org/10.5194/acp-3-161-2003>, 2003.
- Shallcross, D. E., Taatjes, C. A., and Percival, C. J.: Criegee intermediates in the indoor environment: new insights, *Indoor Air*, 24, 495–502, 2014.
- Sheps, L., Scully, A. M., and Au, K.: UV absorption probing of the conformer-dependent reactivity of a Criegee intermediate  $\text{CH}_3\text{CHOO}$ , *Phys. Chem. Chem. Phys.*, 16, 26701–26706, 2014.
- Sheps, L., Rotavera, B., Eskola, A. J., Osborn, D. L., Taatjes, C. A., Au, K., Shallcross, D. E., Khan, M. A. H., and Percival, C. J.: The reaction of Criegee intermediate  $\text{CH}_2\text{OO}$  with water dimer: primary products and atmospheric impact, *Phys. Chem. Chem. Phys.*, 19, 21970–21979, 2017.
- Sindelarova, K., Granier, C., Bouarar, I., Guenther, A., Tilmes, S., Stavrou, T., Müller, J.-F., Kuhn, U., Stefani, P., and Knorr, W.: Global data set of biogenic VOC emissions calculated by the MEGAN model over the last 30 years, *Atmos. Chem. Phys.*, 14, 9317–9341, <https://doi.org/10.5194/acp-14-9317-2014>, 2014.
- Singer, B. C., Coleman, B. K., Destailhats, H., Hodgson, A. T., Lunden, M. M., Weschler, C. J., and Nazaroff, W. W.: Indoor secondary pollutants from cleaning product and air freshener use in the presence of ozone, *Atmos. Environ.*, 40, 6696–6710, 2006a.
- Singer, B. C., Destailhats, H., Hodgson, A. T., and Nazaroff, W. M.: Cleaning products and air fresheners: emissions and resulting concentrations of glycol ethers and terpenoids, *Indoor Air*, 16, 179–191, 2006b.
- Sipilä, M., Jokinen, T., Berndt, T., Richters, S., Makkonen, R., Donahue, N. M., Mauldin III, R. L., Kurtén, T., Paasonen, P., Sarnela, N., Ehn, M., Junninen, H., Rissanen, M. P., Thornton, J., Stratmann, F., Herrmann, H., Worsnop, D. R., Kulmala, M., Kerminen, V.-M., and Petäjä, T.: Reactivity of stabilized Criegee intermediates (sCIs) from isoprene and monoterpene ozonolysis toward  $\text{SO}_2$  and organic acids, *Atmos. Chem. Phys.*, 14, 12143–12153, <https://doi.org/10.5194/acp-14-12143-2014>, 2014.
- Smith, M. C., Chao, W., Takahashi, K., Boering, K. A., and Lin, J. J.-M.: Unimolecular Decomposition Rate of the Criegee Intermediate  $(\text{CH}_3)_2\text{COO}$  Measured Directly with UV Absorption Spectroscopy, *J. Phys. Chem. A*, 120, 4789–4798, <https://doi.org/10.1021/acs.jpca.5b12124>, 2016.
- Su, Y.-T., Lin, H.-Y., Putikam, R., Matsui, H., Lin, M. C., and Lee, Y.-P.: Extremely rapid self-reaction of the simplest Criegee intermediate  $\text{CH}_2\text{OO}$  and its implications in atmospheric chemistry, *Nat. Chem.*, 6, 477–483, 2014.
- Taatjes, C. A., Welz, O., Eskola, A. J., Savee, J. D., Osborn, D. L., Lee, E. P. F., Dyke, J. M., Mok, D. W. K., Shallcross, D. E., and Percival, C. J.: Direct measurements of Criegee intermediate  $(\text{CH}_2\text{OO})$  formed by reaction of  $\text{CH}_2\text{I}$  with  $\text{O}_2$ , *Phys. Chem. Chem. Phys.*, 14, 10391–10400, 2012.
- Taatjes, C. A., Welz, O., Eskola, A. J., Savee, J. D., Scheer, A. M., Shallcross, D. E., Rotavera, B., Lee, E. P. F., Dyke, J. M., Mok, D. W. K., Osborn, D. L., and Percival, C. J.: Direct Measurements of Conformer-Dependent Reactivity of the Criegee Intermediate  $\text{CH}_3\text{CHOO}$ , *Science*, 340, 177–180, 2013.
- Taatjes, C. A., Shallcross, D. E., and Percival, C. J.: Research frontiers in the chemistry of Criegee intermediates and tropospheric ozonolysis, *Phys. Chem. Chem. Phys.*, 16, 1704–1718, 2014.
- Taipale, R., Sarnela, N., Rissanen, M., Junninen, H., Rantala, P., Korhonen, F., Siivola, E., Berndt, T., Kulmala, M., Mauldin III, R. L., Petäjä, T., and Sipilä, M.: New instrument for measuring atmospheric concentrations of non-OH oxidants of  $\text{SO}_2$ , *Boreal Environ. Res.*, 19 (suppl. B), 55–70, 2014.
- Truhlar, D. G., Garrett, B. C., and Klippenstein, S. J.: Current Status of Transition-State Theory, *J. Phys. Chem.*, 100, 12771–12800, 1996.
- Vereecken, L.: The Reaction of Criegee Intermediates with Acids and Enols, *Phys. Chem. Chem. Phys.*, 19, 28630–28640, <https://doi.org/10.1039/C7CP05132H>, 2017.
- Vereecken, L. and Francisco, J. S.: Theoretical studies of atmospheric reaction mechanisms in the troposphere, *Chem. Soc. Rev.*, 41, 6259–6293, 2012.
- Vereecken, L. and Nguyen, H. M. T.: Theoretical Study of the Reaction of Carbonyl Oxide with Nitrogen Dioxide:  $\text{CH}_2\text{OO} + \text{NO}_2$ , *Int. J. Chem. Kinet.*, 49, 752–760, 2017.
- Vereecken, L. and Peeters, J.: The 1,5-H-shift in 1-butoxy: A case study in the rigorous implementation of transition state theory for a multirotamer system, *J. Chem. Phys.*, 119, 5159–5170, 2003.
- Vereecken, L., Harder, H., and Novelli, A.: The reaction of Criegee intermediates with  $\text{NO}$ ,  $\text{RO}_2$ , and  $\text{SO}_2$ , and their fate in the atmosphere, *Phys. Chem. Chem. Phys.*, 14, 14682–14695, 2012.
- Vereecken, L., Harder, H., and Novelli, A.: The reactions of Criegee intermediates with alkenes, ozone and carbonyl oxides, *Phys. Chem. Chem. Phys.*, 16, 4039–4049, 2014.
- Vereecken, L., Rickard, A. R., Newland, M. J., and Bloss, W. J.: Theoretical study of the reactions of Criegee intermediates with ozone, alkylhydroperoxides, and carbon monoxide, *Phys. Chem. Chem. Phys.*, 17, 23847–23858, 2015.
- Vereecken, L., Novelli, A., and Taraborrelli, D.: Unimolecular decay strongly limits concentration of Criegee intermediates in the atmosphere, *Phys. Chem. Chem. Phys.*, 19, 31599–31612, <https://doi.org/10.1039/C7CP05541B>, 2017.
- Wang, L. and Wang, L.: Mechanism of gas-phase ozonolysis of sabinene in the atmosphere, *Phys. Chem. Chem. Phys.*, 19, 24209–24218, <https://doi.org/10.1039/c7cp03216a>, 2017.
- Wei, W., Zheng, R., Pan, Y., Wu, Y., Yang, F., and Hong, S.: Ozone Dissociation to Oxygen Affected by Criegee Intermediate, *J. Phys. Chem. A*, 118, 1644–1650, 2014.
- Wei, W.-M., Yang, X., Zheng, R.-H., Qin, Y.-D., Wu, Y.-K., and Yang, F.: Theoretical studies on the reactions of the simplest Criegee intermediate  $\text{CH}_2\text{OO}$  with  $\text{CH}_3\text{CHO}$ , *Comp. Theor. Chem.*, 1074, 142–149, 2015.
- Welz, O., Savee, J. D., Osborn, D. L., Vasu, S. S., Percival, C. J., Shallcross, D. E., and Taatjes, C. A.: Direct Kinetic Measurements of Criegee Intermediate  $(\text{CH}_2\text{OO})$  Formed by Reaction of  $\text{CH}_2\text{I}$  with  $\text{O}_2$ , *Science*, 335, 204–207, 2012.

- Welz, O., Eskola, A. J., Sheps, L., Rotavera, B., Savee, J. D., Scheer, A. M., Osborn, D. L., Lowe, D., Murray Booth, A., Xiao, P., Anwar H., Khan, M., Percival, C. J., Shallcross, D. E., and Taatjes, C. A.: Rate coefficients of C1 and C2 Criegee intermediate reactions with formic and acetic acid near the collision limit: direct kinetics measurements and atmospheric implications, *Angew. Chem. Int. Edit.*, 53, 4547–4750, 2014.
- Winterhalter, R., Neeb, P., Grossmann, D., Kolloff, A., Horie, O., and Moortgat, G.: Products and Mechanism of the Gas Phase Reaction of Ozone with  $\beta$ -pinene, *J. Atmos. Chem.*, 35, 165–197, 2000.
- Yao, L., Ma, Y., Wang, L., Zheng, J., Khalizov, A., Chen, M., Zhou, Y., Qi, L., and Cui, F.: Role of stabilized Criegee Intermediate in secondary organic aerosol formation from the ozonolysis of  $\alpha$ -cedrene, *Atmos. Environ.*, 94, 448–457, 2014.
- Zhang, D. and Zhang, R.: Ozonolysis of  $\alpha$ -pinene and  $\beta$ -pinene: Kinetics and mechanism, *J. Chem. Phys.*, 122, 114308, <https://doi.org/10.1063/1.1862616>, 2005.
- Zhang, J., Huff Hartz, K. E., Pandis, S. N., and Donahue, N. M.: Secondary Organic Aerosol Formation from Limonene Ozonolysis: Homogeneous and Heterogeneous Influences as a Function of  $\text{NO}_x$ , *J. Phys. Chem. A*, 110, 11053–11063, 2006.